



Contents lists available at ScienceDirect

The Crop Journal

journal homepage: www.elsevier.com/locate/cj

A comprehensive study of the proteins involved in salinity stress response in roots and shoots of the FL478 genotype of rice (*Oryza sativa* L. ssp. *indica*)

Camilo López-Cristoffanini^{a,*}, Mireia Bundó^b, Xavier Serrat^a, Blanca San Segundo^{b,c}, Marta López-Carbonell^a, Salvador Nogués^a

^aDepartament de Biologia Evolutiva, Ecologia i Ciències Ambientals, Secció de Fisiologia Vegetal, Universitat de Barcelona, 08028 Barcelona, Spain

^bCentre for Research in Agricultural Genomics (CRAG), CSIC-IRTA-UAB-UB, Edifici CRAG, Campus de la UAB, 08193 Bellaterra, Barcelona, Spain

^cConsejo Superior de Investigaciones Científicas (CSIC), Barcelona, Spain

ARTICLE INFO

Article history:

Received 3 April 2020

Revised 17 October 2020

Accepted 27 November 2020

Available online 18 December 2020

Keywords:

FL478

Shotgun proteomics

Rice

Salinity

Root

Saltol

ABSTRACT

Rice, a major staple, is the most salt-sensitive cereal. High salinity triggers several adaptive responses in rice to cope with osmotic and ionic stress at the physiological, cellular, and molecular levels. A major QTL for salinity tolerance, named *Saltol*, is present on chromosome 1 of Indian landraces such as Pokkali and Nona Bokra. The early proteomic and physiological responses to salinity in roots and shoots of FL478, an inbred rice line harboring the *Saltol* QTL, were characterized. Plantlets were cultured in hydroponic cultures with 100 mmol L⁻¹ NaCl and evaluated at 6, 24, and 48 h. At the physiological level, root length significantly increased at 48 h, whereas shoot length was reduced. The Na⁺/K⁺ ratio was maintained at lower levels in shoots than in roots, suggesting that roots play a protective role. More than 2000 proteins were detected in both tissues. Roots showed a faster and more coordinated proteomic response than shoots, evident after only 6 h of treatment. These responses showed clear correspondence with those of proteins involved in transcription and translation. Maintenance of mitochondrial activity and amino acid metabolism in roots, and activation of stress-responsive proteins such as dehydrins and PLAT in shoots, may play a key role during the response of the plant to salinity stress. Proteomic and physiological responses showed that roots respond in a more highly adaptive manner than shoots to salinity stress, suggesting that this tissue is critical to the tolerance observed in cultivars harboring *Saltol*.

© 2020 2021 Crop Science Society of China and Institute of Crop Science, CAAS. Production and hosting by Elsevier B.V. on behalf of KeAi Communications Co., Ltd. This is an open access article under the CC BY-NC-ND license (<http://creativecommons.org/licenses/by-nc-nd/4.0/>).

1. Introduction

Rice is the most salt-sensitive cereal worldwide and is classified as a glycophyte [1]. The seedling and reproductive stages of rice are the most sensitive to salinity stress, with exposure leading to yield losses [1–4]. Salinity stress in the crop triggers several adaptive responses at the molecular, cellular, metabolic, and physiological levels to cope with the osmotic and ionic stress that excessive salt incurs [5–7]. These responses mainly involve ion homeostasis in the form of reduced salt intake through roots and efficient intracellular compartmentation and transport of salts to vacuoles or to the external medium. Other typical responses to salinity stress are antioxidant metabolism activation, protein modifications, and increases in energy and biomolecule metabolism [1,3,6,8]. Reddy

et al [1] and Roy et al. [9] propose three main mechanisms: (i) tissue tolerance, (ii) osmotic tolerance, and (iii) ion exclusion. All these mechanisms allow plants to withstand salt stress. In fact, Djanaguiraman et al. [10] showed that salt-tolerant rice accessions have higher rates of germination, greater shoot and root lengths, and a higher vigor index. It has also been observed [1,6,11] that landraces, local cultivars, have greater tolerance to salinity owing to their height, which allows them to dilute the Na⁺ content in their cells, even if their net transport of Na⁺ is comparable to that of high-yielding cultivars.

Rice tolerance to salinity has been widely and thoroughly studied in shoots and more than 70 QTL have been identified with this trait in several cultivars and accessions [12–14]. Because the majority of salinity tolerance mechanisms regulate ion homeostasis, the majority of QTL have been associated with Na⁺/K⁺ transport, exclusion, and compartmentation [12,14,15]. Zhang et al. detected a QTL involved in salt tolerance on chromosome 7 of a

* Corresponding author.

E-mail address: camilo.lopez.cr.puc@gmail.com (C. López-Cristoffanini).

mutant line, M-20, which originated from plating anthers of a semi-sensitive cultivar, 77–170, on a medium containing NaCl [16]. Later, Gong et al. [17] and Prasad et al. [18] mapped QTL for salt tolerance on chromosomes 1 and 6, respectively. In 2001, one QTL for Na uptake, two QTL for Na⁺ concentration, and one QTL for the Na⁺:K⁺ ratio were identified in a mapping population designated IR55178 (from a cross between IR4630 and IR15324) [19]. Bonilla et al. [20] found in a Pokkali (IRGC 108921)/IR29 (IRGC 30412) recombinant inbred line (RIL) population a QTL that explained more than 70% of the variation in salt uptake during salt stress, this being caused by high K⁺ and low Na⁺ absorption and thus a low Na⁺/K⁺ ratio [20–23]. From this RIL population, the FL478 (*Oryza sativa* L. ssp. *indica*) line was developed, which has high levels of seedling-stage salinity tolerance, lacks photoperiod sensitivity, and is shorter in height and life cycle than the original salt-tolerant Pokkali landrace [24]. Similarly, Lin et al. [12] found in crosses between Nona Bokra and Koshihikari a QTL that explained more than 48% of the phenotypical variance caused by an accumulation of K⁺ in shoots during salinity stress. In fact, the QTL from both the RIL and Nona Bokra/Koshihikari populations can be mapped close together on rice chromosome 1, in a region containing the *Saltol* QTL, which is derived from landraces known to be salt-tolerant, such as Pokkali and Nona Bokra [6,11,12,20,23]. Within this region, genes encoding for *OshKT1;5*, *SALT*, peroxidases (PDXs), wall-associated kinases, and protein kinases have been identified along with several transcription factors [25–29]. There is substantial evidence [11,30,31] that the key gene conferring high tolerance to salinity in this region is the *OshKT1;5* gene (formerly called *OshKT8* and *SKC1*), which encodes the cation transporter HKT8, an HKT-type transporter.

The benchmark discovery of the *OshKT1;5* gene has led to an increase in studies of accessions that carry this salinity tolerance allele, such as Pokkali, Nona Bokra, and the RIL FL478. The approaches taken to investigate this gene's involvement in salinity tolerance have included physiological studies, transcriptomics, and proteomics [3,8,11,32–36]. The gene was isolated and studied in detail by Ren et al. [33] to understand its molecular basis. Their conclusion, based on rice mRNA expression and voltage clamping of *Xenopus laevis* oocytes, was that *OshKT1;5* acts in the recirculation of Na⁺ by unloading it from the xylem, where the gene is mainly expressed, and delivering it to the roots, avoiding its accumulation in shoots. *OshKT1;5* physiology was studied in detail in two T-DNA insertional mutants in which it was shown to be present in roots and its major role was to prevent Na⁺ accumulation in shoots [37], as also observed by Ren et al. [33]. Using an Affymetrix rice genome array containing 55,515 probe sets, Walia et al. [35] found no evidence for the gene's expression in shoots. Similarly, Lakra et al. [8] detected expression of a similar gene, *OshKT1;1*, only in shoots, by means of qRT-PCR. When *Saltol* was introgressed into Pusa Basmati 1121, *OshKT1;5* expression was detected in the resulting lines by qPCR approximation showing differential patterns among lines [38].

The main objective of the present study was to characterize the proteome of FL478 in both roots and shoots, a salt-tolerant elite line that carries the *Saltol* region, during early salinity stress. A shotgun proteomic approach was employed that allowed the identification of hydrophobic proteins and proteins of low abundance that are masked in conventional 2D-PAGE [39,40]. In addition, a physiological characterization was performed in roots and shoots of FL478.

2. Materials and methods

2.1. Plant material and hydroponic culture

Seeds of the salt-tolerant cultivar FL478 (IR66946-3R-178-1-1; *Oryza sativa* L. ssp. *indica*) were obtained from IIRRI (International

Rice Research Institute, Los Baños, Laguna, the Philippines). For hydroponic assays, seeds were sterilized first in 70% ethanol for 3 min and then in 40% sodium hypochlorite solution supplemented with 0.02% Tween-20 for 30 min and finally washed five times in sterile water. Seeds were germinated on a Petri dish containing a sterile filter paper previously soaked with sterile water for 7 days at 28 ± 0.5 °C and 166.05 μmol m⁻² s⁻¹ fluorescent light under a 12 h/12 h light/darkness photoperiod. Each seedling was placed in one precut foam plug (2 × 2 × 1 cm, width × length × height) inserted into a hole in a floating rectangular platform (17 × 25 × 2 cm, width × length × height). Each platform was made of extruded polystyrene with 24 holes of 2 cm diameter. Two platforms were positioned in one container filled with 10 L of modified Yoshida solution (Table S1) [41]. All seedlings were grown in a greenhouse with temperature and humidity control (25 ± 3 °C and 50% ± 10% RH) for 1 week for plantlet acclimatization. For the salinity and mock treatments, the hydroponic solution was supplemented with or without 100 mmol L⁻¹ NaCl. Salinity in each container was measured with a DiST 4 Waterproof EC Tester (Hanna Instruments, Woonsocket, RI, USA) with initial conductances of respectively 1.13 ± 0.05 and 9.28 ± 0.10 mS cm⁻¹ being registered in the mock and salinity treatments. Samples were collected at three time points (6, 24, and 48 h) in both mock and salinity treatments, using a randomized block design for all six containers. At the time of sample collection, shoots and roots were separated and sets of four plantlets were quickly rinsed with MilliQ water to remove excess salt and rapidly frozen in liquid nitrogen, and then stored at –80 °C until required.

2.2. Physiological characterization

Plant traits were recorded at 6, 24, and 48 h after mock or salinity treatment. Relative chlorophyll content (SPAD units) was quantified with a SPAD-502 (SPAD MCL502, Minolta, Osaka, Japan). Growth was determined using whole plantlet length and whole plantlet fresh weight, as well as length and fresh weight of shoots and roots. Fresh weight was recorded for groups of four plantlets before MilliQ rinsing. Prior to sample freezing, each group was photographed and the lengths were measured with ImageJ 1.50i (National Institutes of Health, Bethesda, MD, USA). Water content (reported as WC (%)) = (weight of fresh sample – weight of dried sample)/weight of fresh sample × 100) was determined for shoots and roots to compare the osmotic effect of the salinity treatment between samples. For this, samples were dried for 72 h in an oven at 70 °C and weighed every 24 h to ensure complete drying. Dried samples were also used to quantify Na⁺ and K⁺ using acid digestion of shoots and roots. The procedure consisted of complete digestion with 2 mL of 67%–69% HNO₃ (J.T. Baker–Fisher Scientific, Pittsburgh, PA, USA) and 1 mL of 30% H₂O₂ (Merck Millipore, Darmstadt, Germany) for 12 h at 90 °C. Samples were then reconstituted with 25 mL of H₂O and optical absorbances were measured with an Optima 8300 ICP-OES spectrometer (Perkin Elmer, Wellesley, MA, USA) at wavelengths (λ) of 589.592 nm for Na⁺ and 766.490 nm for K⁺.

2.3. Protein sample preparation

Protein extraction was performed in triplicate, for shoots and roots, following Kim et al. [42]. This method incorporates a RuBisCO depletion step using protamine sulfate, as removing this abundant protein allows identifying low-abundance proteins [39,42,43]. This step was performed only for shoots, as RuBisCO is not present in rice roots [44]. Protein concentrations were determined with the Bradford reagent (Bio-Rad Laboratories, Hercules, CA, USA). Extracted shoot and root proteins were stored in 80% acetone at –20 °C until further use [42].

2.4. Protein digestion

Samples stored in 80% acetone were centrifuged to remove acetone and compact the precipitate. The precipitate was resuspended in 700 μL 8 mol L^{-1} urea supplemented with 50 mmol L^{-1} ammonium bicarbonate (AB), and disaggregated and solubilized (UP200S ultrasonic processor (Hielscher Ultrasonics, Teltow, Germany), 20% amplitude, 0.1 cycles, 45 min). Disaggregated samples were cleaned in a particle filter (Corning Costar Spin-X centrifuge tube filters (Corning Inc. Corning, NY, USA), cellulose acetate membrane, pore size 0.45 μm , non-sterile; 9000 \times g, 2 min, room temperature), and the resulting filtrate was designated as the soluble protein fraction for analysis. The volume of this fraction was reduced to 150–200 μL with an Amicon Ultra filter (3 kDa, 0.5 mL, Merck Millipore, Burlington, MA, USA) and then quantified with the Pierce 660 Protein assay (Thermo Fisher Scientific, Waltham, MA, USA).

A total of 35 μg of each sample was made to 400 μL with 50 mmol L^{-1} AB/8 mol L^{-1} urea (pH 8.0–8.5) for digestion using the FASP (Filter-Aided Sample Prep) approach. Samples were reduced with 5.3 mmol L^{-1} Tris-(2-carboxyethyl) phosphine (TCEP) (90 min, 30 $^{\circ}\text{C}$) and alkylated with 27.3 mmol L^{-1} iodoacetamide (30 min in the dark, 30 $^{\circ}\text{C}$). To remove interfering agents, samples were then loaded onto an Amicon Ultra filter (10 kDa, 0.5 mL) and washed by two rounds of centrifugation with 8 mol L^{-1} urea supplemented with 50 mmol L^{-1} AB (13,600 \times g, 25 min, RT, 400 μL), and a final wash with 50 mmol L^{-1} AB (13,600 \times g, 25 min, RT, 400 μL). Protein samples were then digested on the filter in 400 μL of 1 mol L^{-1} urea supplemented with 50 mmol L^{-1} BA plus 2.8 μg of trypsin/sample (sequence-grade modified trypsin (Promega, Madison, WI, USA) for 3 h (32 $^{\circ}\text{C}$, pH 8.0), and redigested for 16 h with 1.4 μg of trypsin/sample (32 $^{\circ}\text{C}$, pH 8.0). The resulting peptide mixtures were recovered with three rounds of centrifugation with washing of the filter with (2 \times) 50 mmol L^{-1} AB (300 μL) and (1 \times) 20% acetonitrile (ACN)/50 mmol L^{-1} AB (200 μL) (13,600 \times g, 25 min). The volume of the peptide solutions was reduced to 300 μL on a SpeedVac (Thermo Fisher Scientific, Waltham, MA, USA) and then acidified with formic acid (FA) (1% final concentration). Acidified peptide solutions were desalted in a C18 tip (P200 Tiptip; PolyLC) per the manufacturer's instructions, dried in a SpeedVac and held at -20°C for subsequent steps. A pool of the analyzed samples (PAS) for shoots and roots was prepared in the same way as the samples used for LC-MS normalization purposes to allow multiple comparison with an Isobaric Tags for Relative and Absolute Quantification (iTRAQ) 8plex Multiplex kit experiment.

2.5. iTRAQ labeling of protein samples

For shoot and root protein samples, three independent iTRAQ experiments were performed, each containing one replicate of the six treatments (two concentrations: 0 and 100 mmol L^{-1} NaCl; three time points: 6, 24, and 48 h) and the PAS. Each iTRAQ experiment consisted of one biological replicate, so that three biological replicates for each tissue, shoots and roots, were analyzed.

Digested and washed samples were resuspended in 30 μL of 500 mmol L^{-1} tetraethylammonium bromide to perform iTRAQ labeling (iTRAQ 8plex Multiplex kit) according to the product specifications. Briefly, 70 μL of isopropanol were added to each vial of iTRAQ labeling reagent and the vials were vortexed for 60 s. The content of each labeled vial was transferred to a sample tube and the tubes were mixed and incubated at room temperature for 2 h to allow the iTRAQ labeling reaction. An aliquot of each reaction was cleaned up with a homemade C18 tip and analyzed with LC-MS/MS to ensure complete labeling before the seven samples in each batch were combined. To each reaction mixture, a volume

of 100 μL of water was added to quench the iTRAQ reaction and labeled samples were combined and dried in a SpeedVac.

Before LCMS/MS analysis, the combined iTRAQ-labeled samples were washed in two steps and then fractionated into 11 fractions, including flowthrough and wash, with a high-pH reversed-phase spin column (Pierce, Thermo Fisher Scientific). In the first cleanup step, the sample was resuspended in 100 μL 1% FA solution, desalted in a C18 tip (P200 Tiptip, PolyLC Inc., Columbia, MD, USA), following the manufacturer's instructions, and dried in a SpeedVac. In the second cleanup step, dried peptides were resuspended in 100 μL 20% ACN supplemented with 0.1% FA (pH 2.7–3.0), cleaned in a strong cationic exchange tip (P200 toptip, PolySULFOETHYL A; PolyLC), according to the instructions, and dried in a SpeedVac. The sample was then subjected to high-pH fractionation with a high-pH reversed-phase peptide fractionation kit (Thermo Fisher Scientific) following the manufacturer's instructions. Briefly, the samples were loaded onto a spin column in 0.1% trifluoroacetic acid (TFA), washed and buffer-exchanged with high-pH buffer and then eluted in nine fractions of increasing ACN concentration (f1 = 10% ACN; f2 = 12.5% ACN; f3 = 15% ACN; f4 = 17.5% ACN; f5 = 20% ACN; f6 = 22.5% ACN; f7 = 25% ACN; f8 = 50% ACN; f9 = 75% ACN). The flowthrough and wash fractions were pooled together, as were fractions one and eight and two and nine, which along with fractions three to seven resulted in eight fractions, which were dried in a SpeedVac.

2.6. LC-MS/MS analysis

The eight dried fractions from each iTRAQ experiment were separated in a liquid chromatograph (nanoAcquity, Waters, Milford, MA, USA) coupled to an LTQ-Orbitrap Velos (Thermo Fisher Scientific) mass spectrometer. The tryptic labeled peptides of each fraction were resuspended in 2% ACN supplemented with 1% FA solution and an aliquot of 10 μL was injected into the chromatograph for separation. Peptides were trapped on a Symmetry C18TM trap column (5 μm \times 180 μm \times 20 mm; Waters) and separated using a C18 reverse-phase capillary column (Acquity UPLC M-Class; 75 μm \varnothing , 25 cm, 1.7 μm BEH column; Waters). The gradient used for peptide elution was 2% to 35% B for 155 min, followed by a 35% to 45% gradient for 20 min (A: 0.1% FA; B: 100% ACN, 0.1% FA), with a 250 nL min^{-1} flow rate. Eluted peptides were subjected to electrospray ionization in an emitter needle (Pico-TipTM, New Objective Inc., Littleton, MA, USA) with an applied voltage of 2000 V. Peptide masses (m/z 300–1800) were recorded in data-dependent mode where a full-scan MS in the Orbitrap was performed with a resolution of 30,000 FWHM at 400 m/z . Up to the 15th most abundant peptide (minimum intensity of 2000 counts) was selected from each MS scan. They were fragmented by higher-energy collision dissociation (HCD) in the C-trap using nitrogen as the collision gas with 40% normalized collision energy, and analyzed in the Orbitrap with a resolution of 7500 FWHM at 400 m/z . The scan time settings were as follows: full MS, 250 ms (1 microscan) and MSn, 300 ms (2 microscans). The generated .raw data files were collected with Thermo Xcalibur V2.2 software (Thermo Fisher Scientific).

2.7. Protein identification

A database was created by merging all entries for *Oryza sativa* ssp. *indica* present in the UniProt database (<http://www.uniprot.org>), with a database containing common laboratory contaminant proteins (Uniprot_Osativa_sub_indica_170405_cont.fasta). Thermo Proteome Discover 1.4.1.14 software (Thermo Fisher Scientific) was used to perform the database search using SequestHT as a search engine. For each iTRAQ experiment, eight .raw files from the MS analyses, corresponding to the eight injected

fractions, were used to perform a single search against this database (enzyme specificity: trypsin; maximum miscleavage sites: 2; fixed modifications: carbamidomethyl of cysteine, iTRAQ8plex [N-term] carbamidomethyl; variable modifications: oxidation of methionine, iTRAQ8plex; peptide tolerance: 10 mg kg⁻¹ and 0.1 Da [respectively for MS and MS/MS spectra]). A search against both a target and a decoy database was performed to obtain a false discovery rate (FDR), and thus estimate the number of incorrect peptide-spectrum matches that exceed a given threshold. A manual search of the NCBI, UniProt, and EBI databases was performed to identify proteins with putatively unknown identity (e.g. uncharacterized proteins) but having a treatment/no-treatment ratio above 2.0 or below 0.5 in at least one of the time points (6, 24, and 48 h), which represents either a two-fold abundance or half abundance of the protein in plantlets subjected to 100 mmol L⁻¹ NaCl. Only those putatively unknown proteins with known regions or domains were added to the identified proteins. To improve database search sensitivity, the Percolator algorithm (a semi-supervised learning machine) was used to aid in the discrimination of correct and incorrect peptide spectrum matches (target FDR (strict): 0.01; validation based on false discovery rate (FDR): $q < 0.01$) [45,46]. Percolator assigns a q -value to each spectrum, which is defined as the minimal FDR at which the identification is deemed correct. These q -values are estimated using the distribution of scores from the decoy database search. A quantification method for iTRAQ 8-plex mass tags optimized for Thermo Scientific Instruments was applied to obtain the reporter ion intensities. The mass spectrometry proteomics dataset of this study is available in the PRIDE partner repository of the ProteomeXchange Consortium, PXD014669 (<http://central.proteomexchange.org/cgi/GetDataset?ID=PX014669>).

2.8. Quantitative analysis and functional annotation

Reporter intensities from the Proteome Discoverer quantitation file were used to perform iTRAQ quantitation. Within each iTRAQ 8plex experiment, reporter ion intensities of each individual peptide from each fraction/LC-MS run were summed. Only unique peptides appearing in all samples of all iTRAQ experiments for either shoots or roots were considered for analysis. To normalize the reporter ion intensities of each label between iTRAQ experiments, a locally weighted scatterplot smoothing (LOWESS) correction was applied using the PAS as an internal standard in each iTRAQ experiment. Following Callister et al. [47], the LOWESS span value was fixed at 0.4. The LOWESS-normalized reporter ion intensities were then divided by their PAS peptide intensities to allow comparison throughout the multi-iTRAQ experiment, for shoots and roots separately. Normalized reporter intensities belonging to a given protein were then averaged to obtain the protein abundance. Proteins were assigned to functional categories according to the GO (Gene Ontology Project, <http://www.geneontology.org>) and KO (KEGG Orthology, <http://www.genome.jp/kegg/ko.html>) databases [48,49].

2.9. Proteomic data visualization

Shotgun proteomics generates large sets of data that are not easily interpreted [50]. Accordingly, to ensure efficient interpretation, several data visualization plots were used: treemaps, volcano plots, protein–protein interaction displays (Cytoscape [51,52] coupled with STRING-DB [53]) and heatmaps. Treemaps are a method for displaying hierarchical data using nested figures that also display quantities by area size [54–56]. This approach was used to illustrate the functional categorization of identified proteins for shoots and roots. Volcano plots are graphs generated by plotting fold-change (using a log₂ transformation) versus P -value ($-\log_{10}$

transformed) of selected quantified proteins. Volcano plots were used for depicting the relative abundances of all the proteins detected in the iTRAQ experiments. In each plot a line crossing the y -axis at 1.301 ($-\log_{10}$ value of the $P = 0.05$, used in the ANOVA analysis, described in section 2.10) was included [50]. Proteins with $P < 0.05$ and $q < 0.15$ for the 100 mmol L⁻¹/0 mmol L⁻¹ (salinity/mock treatment) ratio were displayed as protein–protein interactions, an approach that helps to elucidate the involvement or action of unidentified proteins. For this, Cytoscape 3.6.0 software coupled with stringAPP 1.3.0 (available at the Cytoscape App Store; <http://apps.cytoscape.org/apps/stringapp>) [50,52] was used. STRING (<https://string-db.org/cgi/input.pl>) is a biological database and online resource of known and predicted protein–protein interactions [53]. First, using the UniProt accession IDs of the identified proteins, a network was constructed with confidence (score) cutoff of 0.4 and no additional interactors using stringAPP to retrieve data from STRING. Then, within Cytoscape, each protein was displayed by its abbreviation and colored according to its relative abundance of the 100 mmol L⁻¹/0 mmol L⁻¹ ratio (downregulated (red) to upregulated (blue) in the salinity treatment) averaging the three time points on a log₂ scale. Heatmaps, which organize data sets as matrices without having to summarize the data, were used for visualizing quantitative patterns across proteins and treatments using protein abundance [50,57]. Heatmaps were grouped by the functional categories used in Treemaps and their abundances were reported using colors as for protein–protein visualization.

2.10. Statistical analysis

Prior to statistical analysis, physiological data were tested for normality and homoscedasticity using the Shapiro–Wilk and Levene's robust tests, respectively. All parameters with the exception of Na⁺ content in shoots and roots and SPAD units were suitable for performing ANOVA. For normal and homoscedastic data, a two-way ANOVA (salinity, time and salinity × time) was performed, followed by a post-hoc Tukey's multiple comparison test. For non-homoscedastic data, a Kruskal–Wallis test followed by a Conover–Iman multiple nonparametric pairwise test was applied. For shoot and root water content as well as for shoot and root Na⁺ and K⁺ content, three biological replicates were used for the statistical test. Six biological replicates were used for fresh weight and 36 biological replicates were used for length and SPAD for the corresponding tests. For all tests, differences were considered to be significant at a probability of 5% ($P < 0.05$). Table S2 shows the P and F values for each of the physiological analysis performed.

For shotgun proteomic analysis, the same procedure was used for shoot and root samples. Proteins identified with at least 2 unique peptides were considered for further statistical analysis. From the resulting proteins, variations in abundance were tested by two-way ANOVA (P -value) and corrected for multiple comparisons (q -value) using the false discovery rate (FDR) method [58]. Tukey's honestly significant difference (HSD) test was applied to adjust ANOVA significant differences for multiple comparisons across tested factors (salinity and time). R packages were used for data analysis [59].

3. Results

3.1. Physiological characterization of FL478 during salinity stress

Salinity treatment significantly reduced the overall growth, length (Figs. 1A, S2; Table S2), and fresh weight (Fig. 1D; Table S2) of FL478 plantlets. Shoot length increased during the experiment in both treatments (0 and 100 mmol L⁻¹ NaCl), but salinity treatment significantly reduced growth by 15.6% after

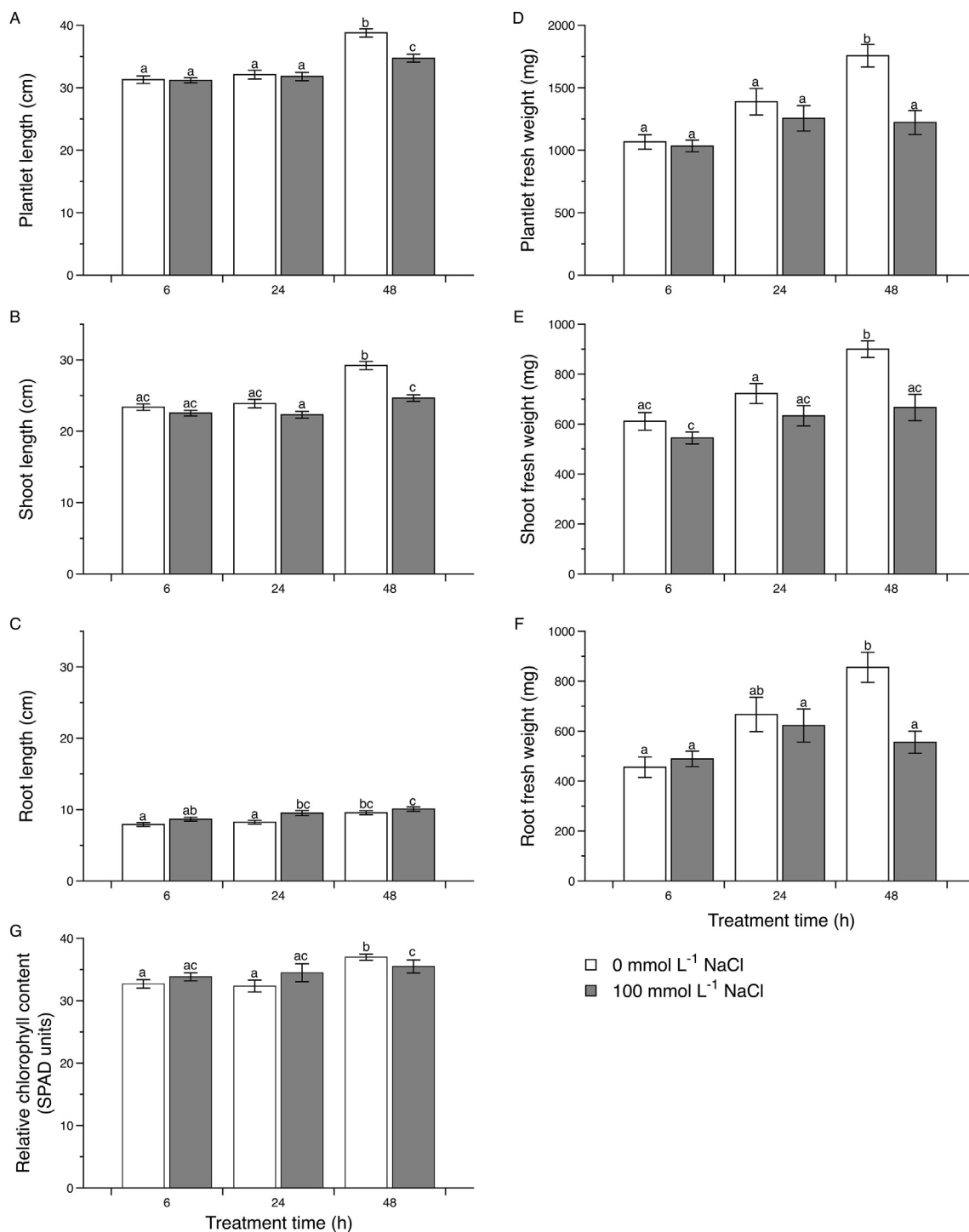


Fig. 1. Physiological characterization of FL478 plantlets in response to different times and concentrations of salinity stress. Fourteen-day-old rice seedlings were subjected to salinity (100 mmol L⁻¹ NaCl) and mock (0 mmol L⁻¹ NaCl) treatment for 6, 24, and 48 h. Growth was monitored by two parameters: length and weight. (A) Plantlet, (B) shoot, and (C) root length values are means ± SE of 36 replicates. (D) Plantlet, (E) shoot, and (F) root fresh weight values are means ± SE of 6 replicates. (G) Relative chlorophyll quantity (SPAD units) values are the mean ± SE of 36 replicates. For plantlet, shoot and root length and fresh weight letters above bars indicate results of Tukey tests; means with the same letter are not significantly different at *P* < 0.05. For SPAD units, letters above bars indicate results of Conover-Iman tests and those with the same letters are not significantly different at *P* < 0.05.

48 h of exposure (Fig. 1B; Table S2). In contrast, root length increased in both treatments and, for the mock treatment, was significantly higher at 48 h than at 24 and 6 h. Salinity treatment caused significant decreases in plantlet, shoot and root fresh weight (Fig. 1D–F; Table S2). For shoot fresh weight, significant differences had already appeared after only 6 h of treatment, whereas

for root fresh weight they started to appear after 24 h. Shoot and fresh weight were significantly different at 48 h between 0 and 100 mmol L⁻¹ NaCl (Fig. 1E and F), and weights corresponded to only 74% and 64% of their respective mock fresh weights, respectively. Relative chlorophyll content (SPAD units) seemed to increase initially in the salinity treatment compared to the mock

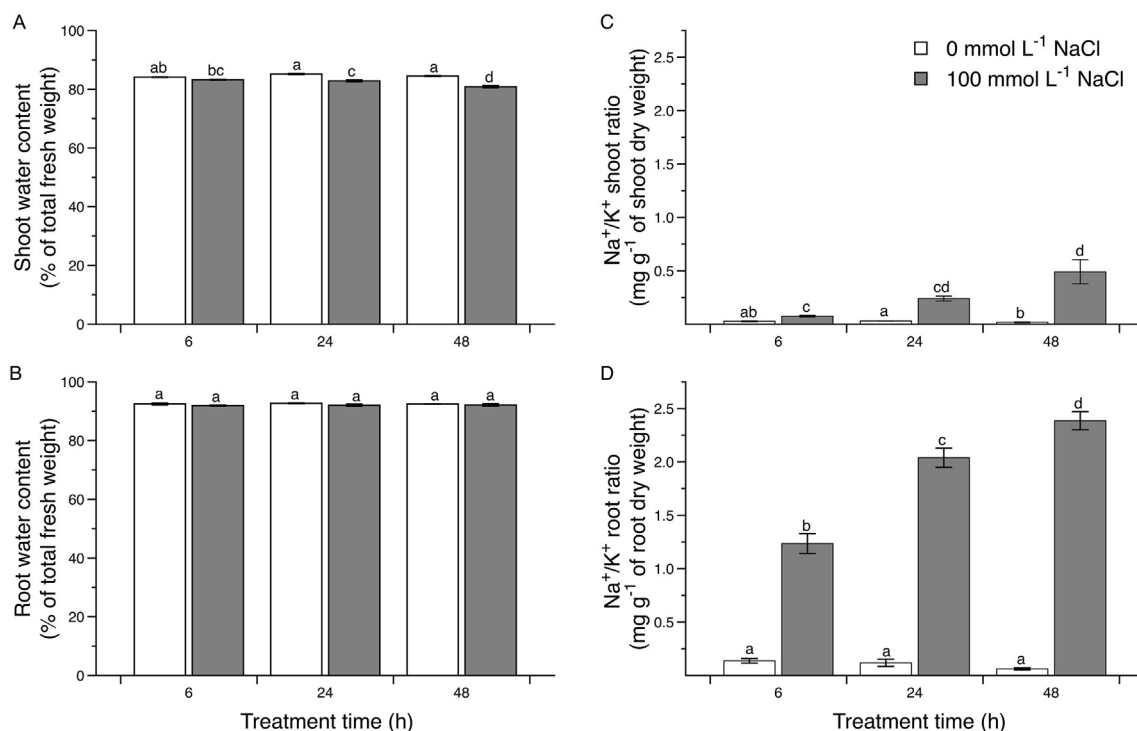


Fig. 2. Shoot (A) and root (B) water content, and shoot (C) and root (D) Na⁺/K⁺ ratio. Values are means \pm SE of 3 replicates. Letters above bars indicate results of Tukey tests for shoot and water content and Na⁺/K⁺ root ratio and Conover-Iman tests for Na⁺/K⁺ shoot ratio; means with the same letters are not significantly different at $P < 0.05$.

treatment, but at 48 h the situation was reversed with relative chlorophyll content being significantly lower in plantlets grown at 100 mmol L⁻¹ NaCl (Fig. 1G; Table S2). Relative chlorophyll content was significantly higher at 48 h under 0 mmol L⁻¹ than in any other treatment (Fig. 1G).

Shoot water content was maintained on average at 84.05% \pm 0.51% for the mock treatment at each time point (Fig. 2A). During the salinity treatment shoot water content was lower at all times, and the difference from the mock treatment was significant at 24 and 48 h (Fig. 2A; Table S2). In contrast, root water content stayed at an average of 92.28 \pm 0.51 in both treatments at all three time points as observed in Fig. 2B, and thus was not influenced by salinity, time, or their interaction (Table S2). The Na⁺/K⁺ ratio in shoots and roots was significantly influenced by salinity \times time interaction, with the concentrations changing owing to salinity and time (Fig. 2C; Table S2). In the mock treatment, the Na⁺/K⁺ ratio showed significant differences in the shoots but at a low level with a mean of 0.025 \pm 0.006. In contrast, in the salinity treatment the Na⁺/K⁺ ratio was significantly higher at 48 h than under all other conditions (Fig. 2C). With the mock treatment in roots, no significant differences were observed. As expected, in the salinity treatment, the Na⁺/K⁺ ratio increased over a longer time and was significantly higher at 48 h than under all other conditions (Fig. 2D). The Na⁺/K⁺ ratio was at least five times higher at all time points in roots than in shoots under salinity treatment.

3.2. Identification and functional categorization of the proteins of the FL478 early proteome under salinity stress

The protamine sulfate RuBisCO depletion protocol was evaluated in SDS-PAGE of shoot proteins. The protocol proved satisfactory, as the RuBisCO large-subunit band was absent in the depleted samples and other bands were more intense than the non-depleted samples (Fig. S1). Accordingly, protein extractions

for shoots and roots under the six conditions (two treatments: 0 and 100 mmol L⁻¹ NaCl; three time points: 6, 24, and 48 h) were performed. By HPLC-MS/MS, respectively 982 and 1116 proteins were identified in shoots and roots, of which 99.2% and 99.6% matched entry proteins in *Oryza sativa* L. ssp. Of all the proteins analyzed, only s148 and s315, shoot proteins, were identified as RuBisCO large and small subunits.

In shoots, 37.2% of the matched proteins corresponded to annotated proteins, while the rest were uncharacterized (full annotated protein list available in Table S3). In roots, annotated proteins comprised 34.3% of the total matched proteins (full list shown in Table S4). During protein identification, subcellular localization was also determined and the cytosol was the most common localization with 85.33% and 91.95% of annotated proteins for shoots and roots, respectively. Among proteins encoded by genes in the *Saltol* QTL region, the *Salt* protein was found only in roots, whereas peroxidase (*PDX*) proteins were found in both shoots and roots. In contrast, the *OsHKT1;5* transporter (previously named *OsHKT8* and *SKC1*), was not detected in either of the tissues.

Finally, functional categorization based on GO and KEGG databases was performed for the 368 and 385 annotated proteins from shoots and roots, respectively (Fig. 3; Tables S3 and S4). Five functional categories were defined: (i) energy and biomolecule metabolism, (ii) genetic and environmental information processing, (iii) antioxidant and defense functions, (iv) cytoskeleton-related, and (v) unassigned function. Each category was further divided into subcategories, as shown in Fig. 3 and Tables S3 and S4. For both tissues, more than half of the proteins, 57.6% on average, were assigned to energy and biomolecule metabolism. This category, also for both tissues, comprised proteins involved in genetic and environmental information processing and antioxidant and defense functions, both showing higher percentages in roots than in shoots. In comparison to shoots, more root proteins were found and assigned to the category of unassigned functions.

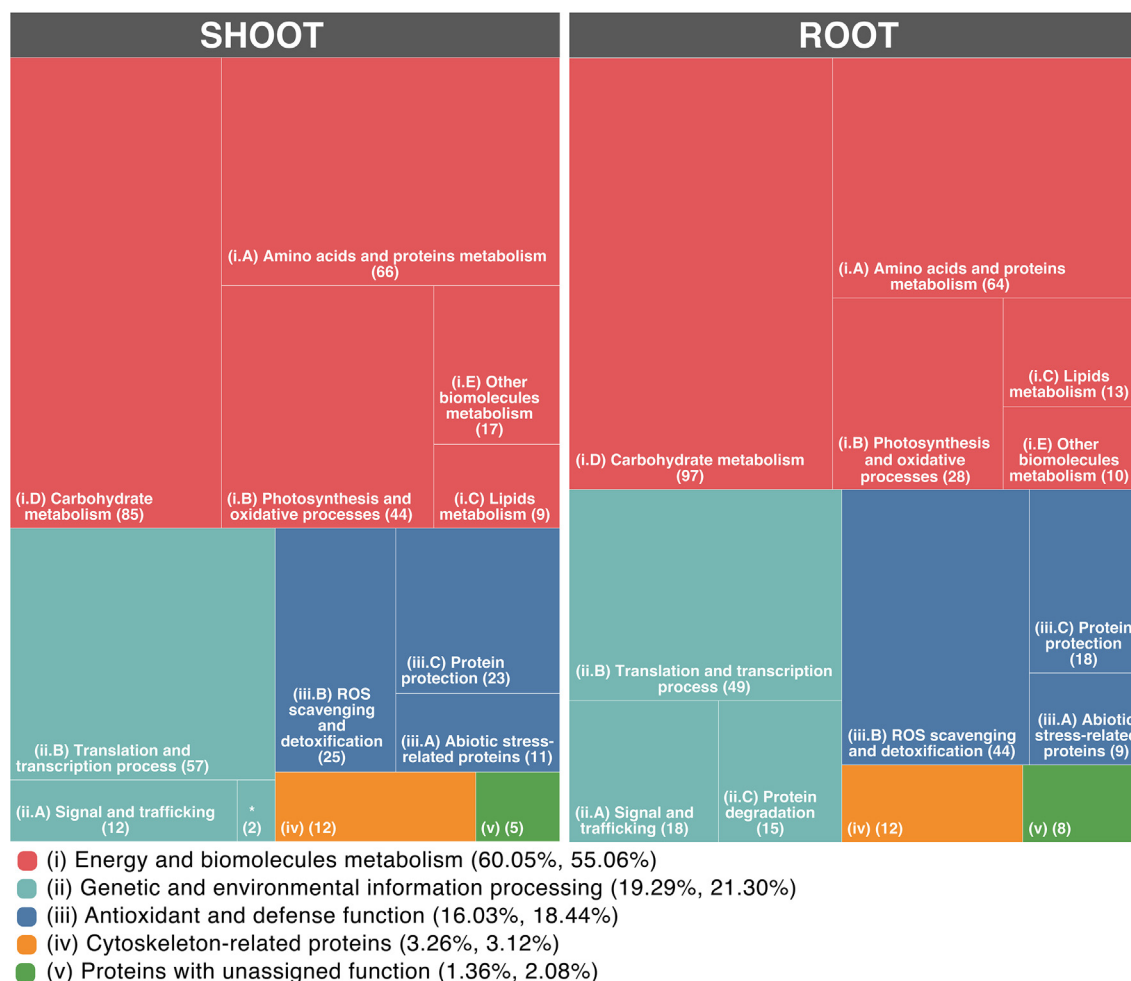


Fig. 3. Treemap showing the functional categorization and subcategorization of proteins from shoots (left) and roots (right). Five functional categories are shown in the legend, where percentages correspond to proteins assigned to each category with respect to total proteins for shoots and roots, respectively. Rectangle sizes are directly proportional to the number of proteins in each subcategory, which are shown in parentheses. *(iii.C) Protein degradation in shoots.

In shoot subcategories, within (i) energy and biomolecule metabolism, the majority of proteins were involved in (i.D) carbohydrate metabolism (mainly glycolysis and the TCA cycle) and (i.A) amino acid and protein metabolism, representing together almost 70% of the proteins in this category (Fig. 3). The next largest subcategory was proteins involved in photosynthesis and oxidative respiration, followed by proteins involved in the metabolism of (i.C) lipids and (i.E) other biomolecules (Fig. 3). Among genetic and environmental information processing proteins, the majority were assigned to (ii.B) translation and transcription processes, representing more than 80.3% of the total in this category. Finally, in the antioxidant and defense functions category, 42.4% and 39.0% were assigned to (iii.B) reactive oxygen species (ROS) scavenging and detoxification, and (iii.C) protein protection.

For root proteins, some similarities with shoots were observed. The main subcategory in (i) was carbohydrate metabolism followed by amino acid and protein metabolism, representing respectively 45.75% and 30.19% in category (i). Many proteins were assigned to translation and transcription processes in roots. The number of root proteins assigned to (ii.C) protein degradation was seven times that in shoots. In roots, as expected, fewer proteins were assigned to the subcategory photosynthesis and oxidative processes (iii.B) than in shoots. Finally, the number of proteins involved in (iii.B) ROS scavenging and detoxification was almost twice that in shoots.

3.3. Global analysis of the early salinity stress proteome of FL478

For this analysis, all proteins matching those in *Oryza sativa* ssp. *indica* were used and their fold-change, as salinity/mock ratio ($100 \text{ mmol L}^{-1} / 0 \text{ mmol L}^{-1} \text{ NaCl}$), was calculated for the three evaluated time points (6, 24, and 48 h) and plotted as volcano plots (Fig. 4). Thresholds for fold-change were established at below 0.8 and above 1.2 corresponding to proteins with lower and higher abundance under salinity treatment. In total, 43 and 36 proteins showed differential abundances ($P < 0.05$) for shoots and roots respectively. Differential abundance was divided equally in shoots, whereas in roots the tendency was of higher abundance under salinity treatment.

The volcano plots in Fig. 4 show that a faster response occurred in roots than in shoots, given that many more proteins showed a significant increase after only 6 h of salinity treatment. In shoots, among 6 h proteins, more than 80% showed no differential abundance and only seven showed significant differential abundances (Fig. 4). This situation was reversed at 48 h, when many more differentially abundant proteins were observed in shoots than in roots. In fact, the number of significantly differential proteins in shoots increased to 58, and only 48% of the proteins showed no differential abundance. Moreover, the fold-change values at 48 h in shoots reached lower than -4 and higher than 3 , whereas in roots the fold-changes remained -1 and 1 as also observed at 6 and 24 h.

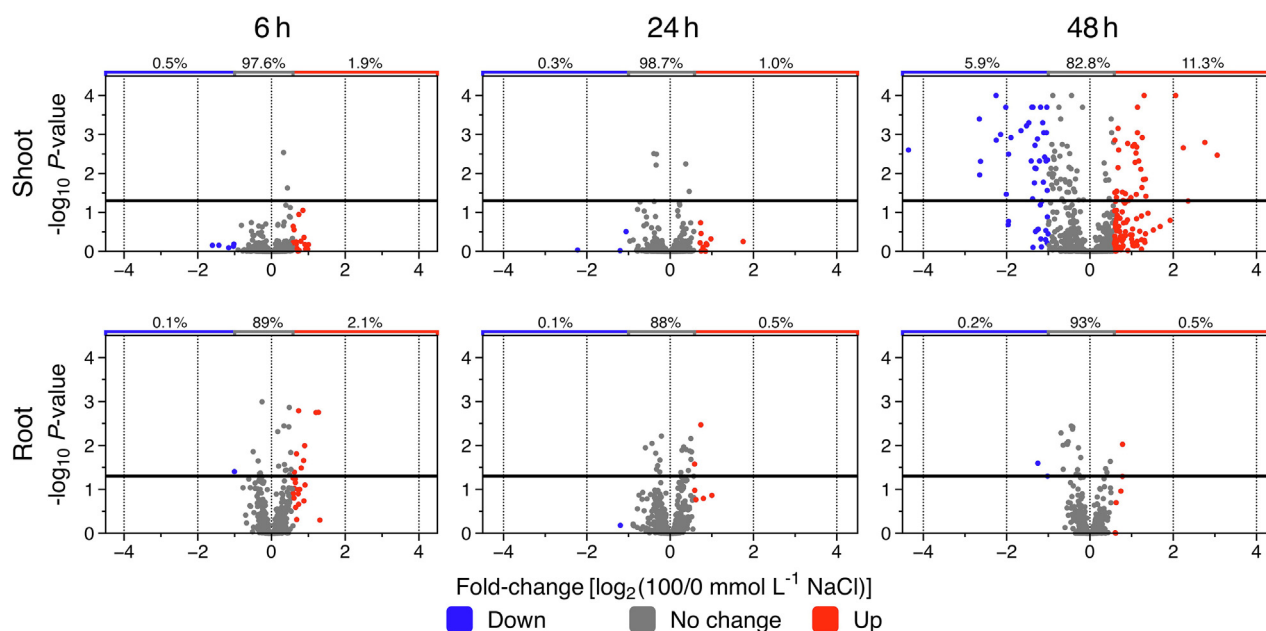


Fig. 4. Volcano plots depicting differential protein abundances in shoots and roots of FL478. Values at the top of each plot indicate the percentage of proteins in each fold-change region. A total of 982 and 1116 proteins are shown at all the time points for shoots and roots, respectively. Values of fold-change are reported as \log_2 of the salinity/mock treatment ($100 \text{ mmol L}^{-1}/0 \text{ mmol L}^{-1} \text{ NaCl}$) ratio for the three time points evaluated (6, 24, and 48 h) where zero corresponds to a salinity/mock ratio of one. The horizontal black line crossing the Y-axis corresponds to 1.301 ($-\log_{10}$ value of $P = 0.05$), and values above that line are significantly different.

Similarly, root protein percentages in each fold-change region were similar between the three time points. The number of root proteins with differential abundance ($P > 0.05$, above black horizontal line in the volcano plots) was similar at the three time points.

3.4. Identification of candidate proteins for salinity tolerance

Among the proteins identified in FL478, 85 shoot and 64 root proteins showed differential abundances ($P < 0.05$) and a low false discovery rate ($q < 0.15$), in comparison with the fold-change averages of the three time points ($100 \text{ mmol L}^{-1}/0 \text{ mmol L}^{-1} \text{ NaCl}$; Table S5). In this subset, some proteins were unknown (not annotated) and were termed UnkS and UnkR for shoots and roots, respectively. Networks established with Cytoscape coupled with STRING-DB are shown in Fig. 5A and B for shoots and roots, respectively. Like the volcano plots, this analysis also demonstrates that the abundance changes in roots were more controlled than those in shoots, given that the fold-changes occupied a narrower range than that for shoots.

The shoot network is interconnected with several clusters of proteins showing substantial abundance changes (-2.7 to 1.27 fold-change), with the majority of proteins being downregulated under salinity (Fig. 5A). PLAT_plant_stress and a plant dehydrin family (DHN) protein, both involved in stress tolerance, showed high abundances under salinity treatment. Two ribosomal proteins (rpuS5 and rps30) showed higher abundances under salinity stress than the mock treatment. The protein UnkS-37, with high abundance under salinity, may be involved in amino acid biosynthesis, given its close links with betaine aldehyde dehydrogenase 2 (BADH2), lysine-tRNA ligase (LysRS), and glutamine amidotransferase (GATase). Proteins UnkS-1, possibly involved in antioxidant and defense functions, and UnkS-13 and UnkS-14 also showed high abundance under salinity treatment. In contrast, three proteins involved in photosynthesis (psbQ, psb27, and LCH) were downregulated, as expected, but another protein involved in this process was upregulated (PsbP). Proteins UnkS-2 and UnkS-35, with unknown function, were significantly less abundant under salinity.

In the root network analysis, UnkR-19 and UnkR-26 showed high abundances during salinity and their connections to histones 2A and 4 (H2A and H4) suggest a role in transcription. A highly interconnected cluster of proteins involved in translation, ribosomal proteins and UnkR-29 and UnkR-4, showed high abundance under the salinity treatment (Fig. 5B). Thus, several of the proteins with no identity are candidates for proteins involved in genetic and environmental information processing. UnkR-17, highly accumulated under salinity, has no known role. It is not related to other proteins but should be investigated further as a potential candidate for salinity tolerance. In contrast, several proteins such as UnkR-9, UnkR-10, and UnkR-24 displayed a pronounced low salinity/mock treatment ratio. No candidate function could be attributed to these proteins, as no interconnection with other proteins was present. Peroxidases (PDXs), of which one gene lies within the *Saltol* region, displayed lower abundances under the salinity treatment.

3.5. Abundance patterns of the early protein stress responses of FL478 under salinity stress

All the proteins identified and listed in Tables S3 and S4 are visually represented in heat maps grouped by the five functional categories, without considering their sub-functional category, for shoots and roots (Figs. S3 and S4, respectively). As observed in Fig. S3, for category (i), energy and biomolecule metabolism, the treatments (0 and $100 \text{ mmol L}^{-1} \text{ NaCl}$) at 48 h clustered separately, evidence of the drastic changes experienced by shoots during the salinity treatment. For this category, several proteins involved in photosynthesis (psbQ, psb27, TSP9, and PSI-N among others) were grouped in clusters 1 and 2 showing low abundance under salinity. In contrast, proteins involved in carbohydrate (e.g. GAPDH and PGK) and amino acid and protein (e.g. CysS and GCS-H) metabolism cluster 4 showed high abundance in salinity. Similar patterns can be observed in category (ii), genetic and environmental information processing, where at 48 h the treatments also clustered separately. Proteins involved in signaling (CaM-1 and annexin among others) in cluster 1 displayed higher abundance at 48 h

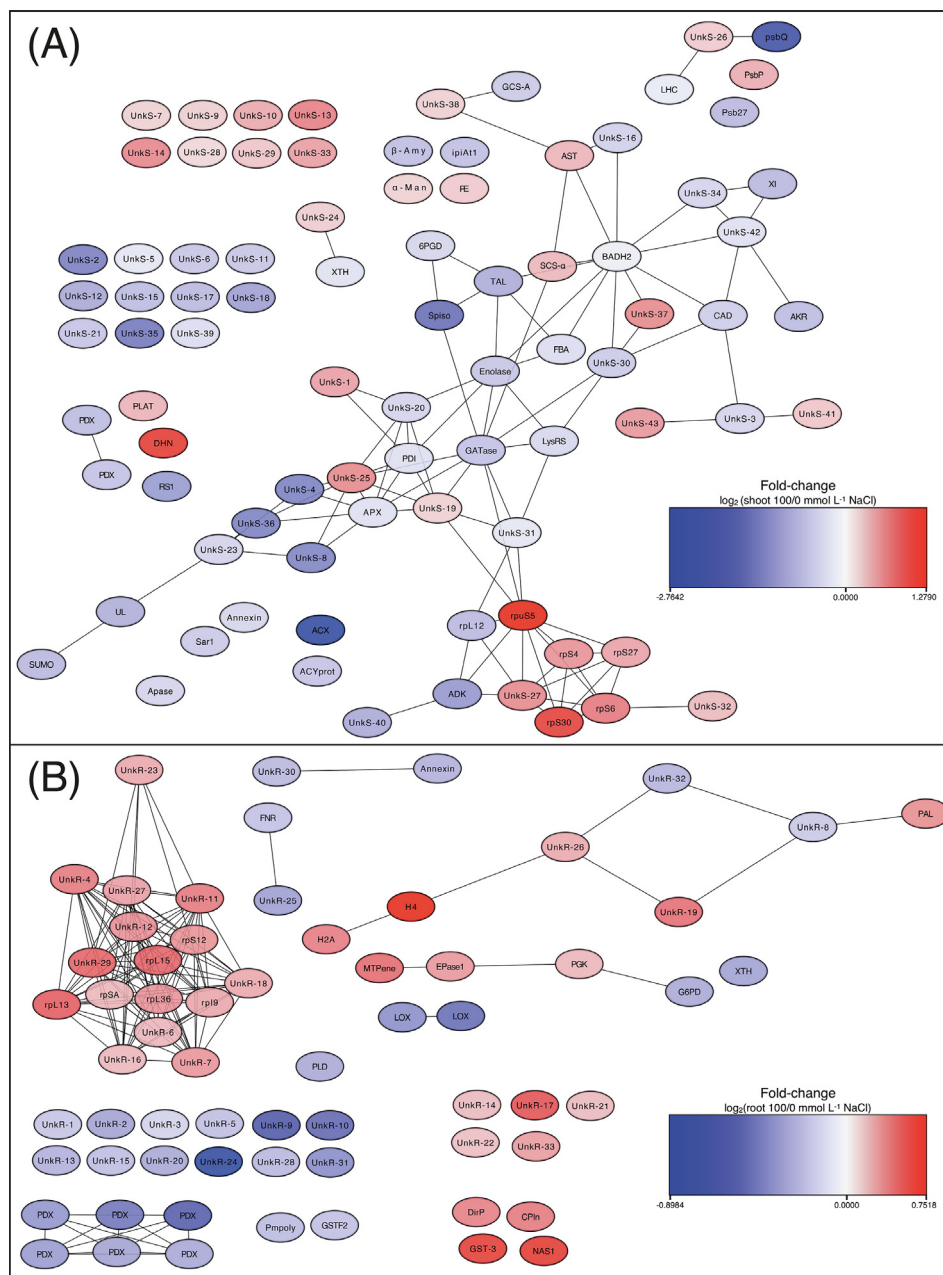


Fig. 5. Shoot (A) and root (B) protein–protein interactions displayed using Cytoscape and Cytoscape’s stringApp. The proteins shown had $P < 0.05$ and $q < 0.15$ for the salinity/mock treatment ($100 \text{ mmol L}^{-1}/0 \text{ mmol L}^{-1} \text{ NaCl}$) ratio. The color of each protein corresponds to the $100 \text{ mmol L}^{-1}/0 \text{ mmol L}^{-1}$ ratio on a \log_2 scale, indicated in the spectrum box of each network. As defined by the software, the length of edges (relationships) between nodes (proteins) indicate the meaningfulness of the protein–protein interactions.

under the mock treatment, whereas the majority of proteins associated with translation and ribosomes in cluster 2 displayed higher abundance under the salinity treatment. As expected for proteins involved in antioxidant and defense functions, category (iii), the mock and salinity treatments were clustered separately with increasing abundances at the three time points. Within this category there were marked differences at 48 h between the mock and salinity treatments. Strikingly, in the case of cluster 3 where an increased abundance at 0 mmol L^{-1} was observed for several enzymes involved in antioxidant stress and protein protection, there was no upregulation of these enzymes at 48 h under $100 \text{ mmol L}^{-1} \text{ NaCl}$. In contrast, there was a reverse of these dynamics for cluster 2 and 4, with these proteins showing increased abundance during the salinity treatment. In the heat

maps of functional categories (iv) and (v), cytoskeleton-related and unassigned function, respectively, there are no clear patterns that correspond to the stress experienced by the plants, but in both categories the treatments (0 and $100 \text{ mmol L}^{-1} \text{ NaCl}$) were grouped separately after hierarchical clustering, as seen for category (ii).

In roots, five clusters were defined within category (i), energy and biomolecule metabolism, as observed in Fig. S4. In contrast to the situation in shoots, at 48 h the two treatments were grouped together, indicating that there were no large differences in this proteome subset in roots during the salinity treatment. In fact, the largest differences between the treatments (0 and $100 \text{ mmol L}^{-1} \text{ NaCl}$) were observed at 24 h in all clusters (Fig. S4). Although a large increase in protein abundance was observed for

carbohydrate and amino acid and protein metabolism in cluster 5, the abundances of the majority of these proteins were the most different among the six conditions (white circles within the squares). In category (ii), genetic and environmental information processing, the mock and salinity treatments at 48 h were grouped together, showing similar abundances, especially in cluster 2, which includes the majority of proteins associated with translation and ribosomes (Fig. S4). For roots, annexin also displayed lower abundance in comparison with the mock treatment at 48 h. There were marked differences between the 6 and 24 h time points in the salinity treatment for clusters 2 and 4, in which proteins involved in the translation process decreased in abundance from 6 to 24 h. Unlike in shoots, in functional category (iii) the salinity and mock treatments did not cluster together in the roots. Nonetheless, protein abundance patterns at 48 h for clusters 1 and 2, which included several antioxidant proteins, were very similar between treatments. In contrast, in clusters 3 and 4, which contained a majority of proteins involved in protein protection (e.g. PPI and chp60), there was a higher abundance at 48 h under the 100 mmol L⁻¹ NaCl treatment. For the last two functional categories, (iv) and (v), the majority of proteins in all the samples assayed showed abundance ratios close to 1:1 (black color), indicating a low differential abundance between treatments, and the treatments were clustered together.

4. Discussion

In the present study we used the rice cultivar FL478, which carries the region on chromosome 1 containing *Saltol*, a QTL known to confer high salinity tolerance in rice [8,24,60,61]. To our knowledge there is only one study [3] of this rice cultivar's proteome under salinity stress, in which changes were recorded after 16 days of exposure. Ours is also the first study of root salinity using shotgun proteomics. To expand our knowledge of the tolerance of *Saltol* cultivars, we performed proteomic and physiological analysis during salinity stress at early stress stages in both shoots and roots (6, 24, and 48 h after salinity treatment). This study, in which roots were analyzed under salinity, contributes to our resources for studying salinity tolerant rice accessions. Our finding that proteomic and physiological changes were more organized in roots suggests that this tissue better tolerates stress and thus plays a crucial role in salinity tolerance.

4.1. Roots of FL478 show an enhanced physiological response to salinity stress compared to shoots

High salinity causes growth reduction in terms of length and fresh weight. It has been proposed [9] that growth reduction can be triggered by two processes, one responsive to salt shoot accumulation (days to weeks) and the other independent of salt accumulation (minutes to days). The two can be experimentally distinguished because the latter explains effects triggered upon addition of salt before there has been time for salt to accumulate in the shoot. This model was supported in our study, in which the Na⁺/K⁺ ratio in salt-stressed shoots at 24 and 48 h was half that recorded in other studies [8,62] where stress was more prolonged. Abdollah Hosseini et al. [3] observed that in FL478 even after 14 days of salinity treatment the shoot Na⁺/K⁺ ratio was maintained at 0.5, a value similar to our values at 48 h, and this finding suggests that mechanisms are set in motion to prevent Na⁺ accumulation in this tissue. In contrast, the root Na⁺/K⁺ ratio increases continuously during salinity stress. At 48 h we recorded values of ~2.5 and Abdollah Hosseini et al. [3] observed at 14 days values of 3.4. Salinity treatment reduced only the shoot length because roots continued their natural development, to probably find less

saline areas in the growing medium. Growth reduction in terms of fresh weight was observed for both tissues, suggesting lower water availability in roots during salinity stress. Still, root water content was similar between treatments, indicating that the difference could be due to development of thinner roots under the salinity treatment that increase the surface to better cope with the high salinity. In accord with our results, Abdollah Hosseini et al. [3] (14 days of salinity treatment) and Lakra et al. [8] (15 min to 72 h of salinity treatment) reported reduction in length and fresh weight during salinity treatments in rice cultivars carrying *Saltol*. Likewise, Khan and Panda [62] reported reductions in the root fresh weight of a salt-tolerant rice cultivar (*O. sativa* L. cv. *Lunishree*) under salinity stress after 24 h of treatment. The overall growth reduction (in length and weight) can be attributed to a low rate of CO₂ assimilation, a possible consequence of the overabundance of ABAr9, which promotes stomatal closure, as well as the lower abundance of photosynthesis proteins and the reduction in chlorophyll content.

4.2. Shotgun proteomics affords advantages over conventional 2D-PAGE

Shoot and root proteomes have been characterized [63,64] by a shotgun proteomics approach for large-scale and high-throughput protein identification. This technique overcomes the limitations of 2D-PAGE, which include low representation of proteins with high molecular weights, high isoelectric points (pIs), hydrophobic domains, and low abundance [40]. We accordingly detected more proteins than other studies that characterized the proteomes of rice cultivars under salinity [3,8,65]. In comparison with the studies of Abdollah Hosseini et al. [3] and Lakra et al. [8], which used *Saltol* cultivars and classical 2D-PAGE techniques, we found respectively 5 and 17 times more proteins in the shoot [3,8]. The number of identified proteins was similar to or higher than those in other studies using an iTRAQ approach for shoots and roots [66,67], including one using cultivar Pokkali [68]. Although there are iTRAQ studies [69–71] that yielded a higher number of proteins, in those studies the parameters for identifying proteins were not as restrictive as in ours (the mass error was set to 20 mg kg⁻¹ instead of 10 mg kg⁻¹) and it is not clear whether or not peptides found in all samples were used for subsequent analysis. Thus, this study represents an expansion of knowledge of the shoot proteome in cultivars harboring the salinity-tolerance *Saltol* QTL. It also expands our current datasets for root proteomes under salinity, which has not been studied in these cultivars.

4.3. Global proteome abundance shows more efficient response in roots than shoots

The proteomics data are summarized in a schematic of key mechanisms for shoots and roots in Fig. 6A and B, respectively. In general, it can be observed that roots are more responsive to salinity than shoots because their response is faster and more organized (Fig. 4). In fact, protein activation in roots starts at 6 h, whereas in shoots it changes, and drastically, only after 48 h of salinity treatment. These events are not unexpected, as roots are the first organs that sense salinity stress [72]. Our results disagree with those of Yan et al. [72], who showed that upregulation of root proteins under salinity stress was maximized after 72 h of stress, a finding that could be explained by the higher NaCl concentration (150 mmol L⁻¹) that they used. Still, in the present study the root protein abundances were similar between mock and salinity treatments, especially for amino acid biosynthesis pathways, suggesting that normal functions are not strongly disrupted. Also, the activation of proteins involved in stress tolerance was higher in roots than in shoots, allowing higher salinity stress tolerance (Fig. 3).

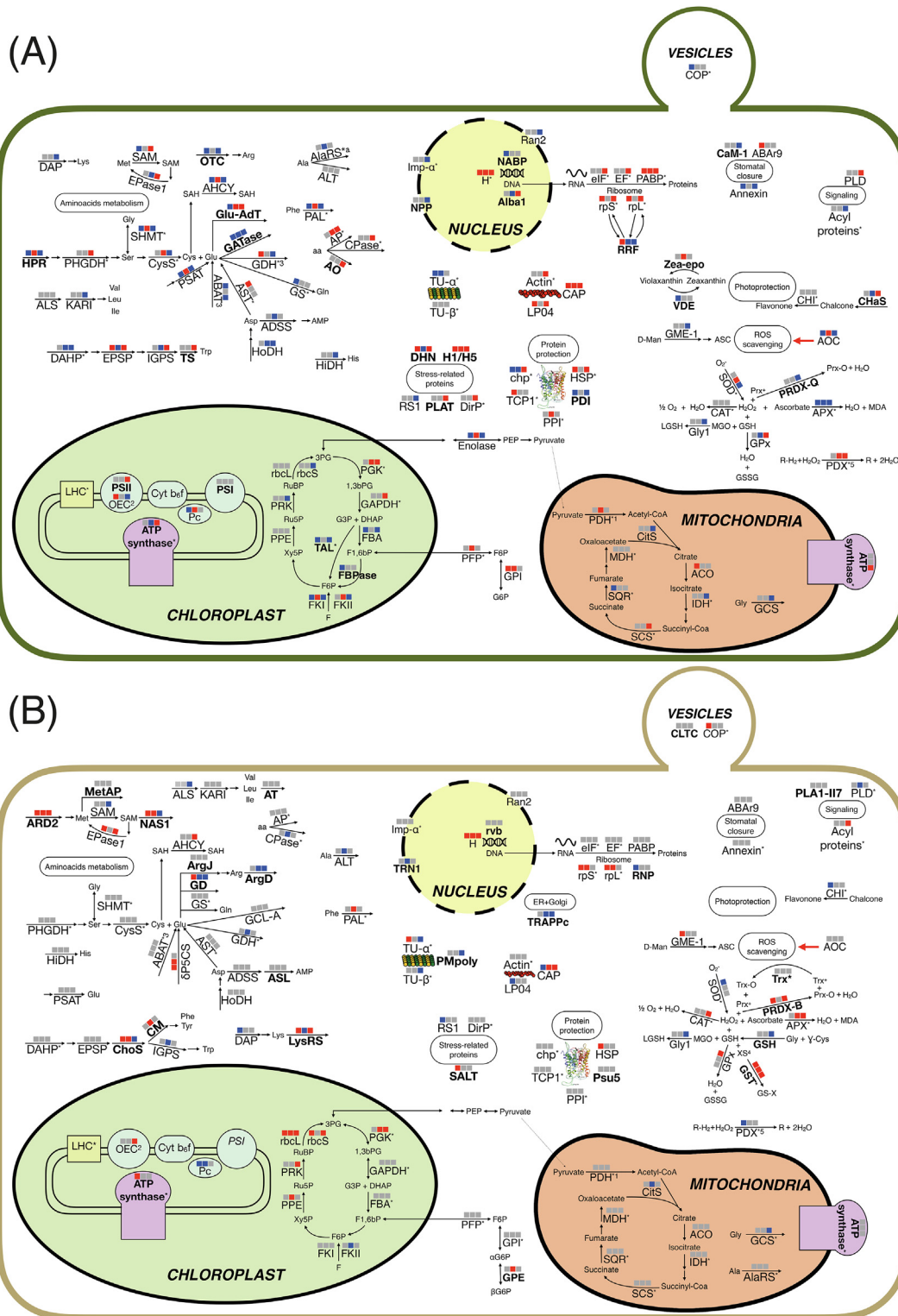


Fig. 6. Cell diagram of the proteins involved in salinity tolerance in shoots (A) and roots (B) of FL478 (abbreviations are according to Tables S3 and S4, respectively). Bold abbreviations correspond to proteins found in either shoots or roots exclusively. The three squares above the protein abbreviations correspond to the abundances at each time (6, 24, and 48 h), calculated as the fold-change in the salinity/mock (100 mmol L⁻¹/0 mmol L⁻¹ NaCl) treatments. Colors in the square correspond to the fold-change: blue denotes down-regulated proteins (<math><0.8</math>), gray denotes no change (0.8–1.2) and red denotes up-regulated proteins (>1.2). *Abundance corresponds to the average of all proteins with the same abbreviation in Tables S3 and S4; ¹corresponds to the average of proteins comprising the pyruvate dehydrogenase complex; ²corresponds to proteins comprising the oxygen-evolving complex; ³corresponds to a mitochondrial protein; ⁴corresponds to xenobiotic substrates; ⁵corresponds to the peroxidase reaction with its optimal substrate (H₂O₂).

We accordingly propose that the more efficient responses displayed by roots in *Saltol*-carrying cultivars are explained by better adaptation to the excessive salt present in the growing medium [9,73].

4.4. Roots and shoots display differential biomolecule and photosynthetic metabolisms when subjected to salinity

The majority of shoot proteins involved in photosynthesis showed lower abundance under the salinity treatment, concomitant with a reduction in relative chlorophyll content values, suggesting a halt in photosynthetic processes. In accord with our findings, Walia et al. [35], Moradi et al. [74], and Lakra et al. [8] showed that photosynthetic CO₂ fixation, stomatal conductance, and transpiration decreased substantially in rice plants exposed to salt stress [8,74]. Although roots are a photosynthetically inactive tissue [44], some photosynthesis-related proteins were identified in root leucoplasts that have been reported [75,76] to be present in other species. Despite the downregulation of the photosynthetic processes, many proteins involved in energy and biomolecule metabolism were upregulated in both tissues, as observed in other studies for shoots [8,65,68] and roots [3]. Greater changes in abundance were observed in shoots than in roots, as also reported by Lakra et al. [68], implying that shoots require more intense activation of cell machinery than roots to avoid salinity-related damage at the plant and cell level. The upregulation of these processes does not greatly increase tolerance to salinity stress itself, but is essential in the activation of pathways involved in producing compatible solutes (e.g. proline and glycinebetaine), triggering antioxidant responses and aiding in signaling cascades for sensing salinity among other functions [6]. For this, a highly coordinated response is required in rice plants, which includes the rapid upregulation of initiation and elongation factors at the transcription and translation levels, as well as many ribosomal proteins needed to activate salinity-tolerance pathways. In fact, our results, along with those of other authors [3,68], show that roots display a more efficient response than shoots.

4.5. Proteins involved in Na⁺ sensing and sequestration and vesicular trafficking

Concerning strategies and mechanisms for coping with excess salt, all plants, even glycophytes (salinity-intolerant plants), have developed the ability to sense the hyperosmotic component and the ionic Na⁺ component of salinity stress [73,77]. This sensing ability depends on a multigene response, and although several genes are already known, the molecular identities of these sensors are not yet elucidated [1,9,73]. Our results contribute to understanding the sensing pathways, as we have identified proteins such as calmodulin, annexin, phospholipases and ABA receptors (Fig. 6A and B). The finding that abundance changes were more prominent in shoots than roots suggest that roots' signaling mechanisms are more consolidated, as Lakra et al. [68] observed for Pokkali under salinity stress. Among these proteins, the transporter OSHK1;5 encoded in the *Saltol* region was not identified under any of the six conditions assayed, as also found by several authors [3,8,32]. High salinity stress rapidly leads to cytosolic Ca²⁺ spiking [7,78], which could strongly influence low-affinity channels called nonselective cation channels that allow Na⁺ to enter cells, and if the channels are not adequately regulated could drastically perturb the Na⁺/K⁺ ratio [1]. Calmodulin is a ubiquitous protein that binds Ca²⁺ and is highly conserved in eukaryotes [78]. As found here and previously [8], it is present in low abundance in shoots during salinity treatments. Loss of function of the *SOS* (Salt Overly Sensitive) gene in *Arabidopsis*, which encodes a Ca²⁺ binding protein, produces mutants that are oversensitive to salt stress [79].

Annexin, a Ca²⁺-dependent phospholipid binding protein, showed higher abundance under salinity than under mock treatment at 48 h in roots and shoots and a high transcriptional activity of this protein accompanied increased stress tolerance [80,81]. Downstream Ca²⁺ kinases could be activated that transduce the perceived signal to activate gene transcription, such as calcium-dependent protein kinases (CDPKs) [73]. Phospholipase D was detected in shoots and roots but exhibited its highest abundance in shoots at 48 h, as observed by Domingo et al. [82] where its transcription was more evident in a salinity-sensitive rice line. This enzyme is involved in the regulation of phospholipid-based signaling, which has been associated with salt stress tolerance, so that its high abundance in shoots could contribute to the salt-tolerance response [82]. ABA is a phytohormone that can play an important role in salinity tolerance by reducing transpirational water loss via stomatal closure [83]. The ABA receptor 9 was over-accumulated only in salt-stressed shoots, suggesting a role in reducing water loss through transpiration by closing stomata, as described previously [84] for other ABA receptors. Several translation-initiation and elongation factors along with many ribosomal proteins were upregulated in shoots and roots. The increase in proteins involved in gene expression has also been reported in rice accessions harboring *Saltol* [3,8], but to our knowledge this is the first time so many proteins involved in this function have been identified.

We also detected other proteins that could be involved in sensing stress signals (hyperosmotic stress and elevated Na⁺ concentration), in particular those involved in vesicular trafficking in cells (clathrin, coatamer, Sar1, secA) and the nucleus (transportin, importin), along with GDI (guanosine nucleotide diphosphate dissociation inhibitor) [85–90]. These proteins showed higher abundance under the salinity treatment, being more abundant in roots than in shoots, in agreement with findings [82,91] that Na⁺ has a low accumulation in shoots in tolerant rice lines. Salinity stress induced bulk-flow endocytosis in *A. thaliana* roots via clathrin-dependent and -independent pathways after only 10 min of exposure to NaCl [92–94]. Luo et al. [95] reported that a gene encoding importin β was required for the drought tolerance response (i.e. the osmotic component of salinity stress). In accord with that study, we observed an increased abundance of importin α in roots after 48 h of 100 mmol L⁻¹ NaCl. Increased vesicular trafficking during salinity stress has been associated [89] with removal of sodium transporters from the plasma membrane, limiting Na⁺ uptake and internalizing of plasma membrane aquaporins to prevent water loss.

4.6. Roots showed higher activation of proteins involved in antioxidant and defense functions than shoots

Higher abundance of proteins involved in oxidative stress, protein protection, and abiotic stress in general was observed in shoots and roots during salinity treatment (Figs. 5A and B, 6A and B). Enzymes involved in ROS scavenging such as ascorbate peroxidase (AP), catalase (CAT), PDX, superoxide dismutase (SOD), and GME-1 (L-ascorbic acid biosynthesis) showed differential higher abundances, suggesting differential activation. In shoots, some protein abundances were lower under the salinity treatment, suggesting an erratic antioxidant response, as Lakra et al. [8,68] observed for Pokkali. The *PDX* gene, contained in the *Saltol* QTL, was substantially upregulated in shoots at 24 and 48 h under 100 mmol L⁻¹ NaCl, whereas in roots its abundance remained the same throughout the treatment, suggesting different roles in the two tissues. In contrast, APX abundances in roots were higher under salinity at the three time points, whereas for shoots lower abundances were observed at 24 and 48 h. SOD, an enzyme involved in ROS scavenging mechanisms, showed higher activity in roots and shoots, as observed by Abdollah Hosseini et al. [3]

for FL478. Li et al. [65] and Dooki et al. [96] reported upregulation of APX and AP in the roots of the rice cultivar 93-11 and the panicles of cultivar IR651, respectively. It appeared in this study, as in others [3,8,68], that antioxidant responses are tissue- and time-specific, given that some enzymes are activated rapidly but others only after prolonged stress, and their responses differ between shoots and roots.

Rice mutants for allene oxide cyclase, a protein downregulated in shoots and roots in the present study, showed increased salt tolerance [97]. Proteins involved in protein protection (e.g. HSPs, peptidylprolyl isomerase, and chaperonins) were markedly upregulated only in shoots, suggesting that roots cope better with salinity and withstand the stress without activating these proteins. Overabundance of chaperonins in roots has been described, but in salinity-sensitive cultivars [98]. As in our study, Lakra et al. [8] found upregulation of a chaperonin for shoot proteins in rice plants harboring *Saltol* (Pokkali). More stress-related proteins were observed in shoots, the majority of them up-regulated, in particular a protein of the dehydrin family (DH) whose members are known [99] to accumulate in rice vegetative tissues. But the Salt protein, encoded in the *Saltol* region, was observed only in roots, in contrast to the findings of Lakra et al. [68], where this protein was not detected under salinity stress in Pokkali using an iTRAQ approach.

The osmotic component of the salt stress can lead to plasmolysis, generating additional stress [23]. We found that cytoskeleton protein abundances between treatments varied greatly in shoots and roots. In general, roots displayed lower abundances than shoots under salinity. Because the cytoskeleton plays a key role in response to high salinity owing to its highly dynamic changes and complex regulatory networks [100], this finding merits further study. Several compatible solutes (osmoprotectants) have been studied in rice [1]. In our study, only two enzymes involved in the synthesis of sucrose (δ P5CS) and glycinebetaine (BADH2), showing higher abundances in roots under salinity stress. In shoots, BADH2 abundance was lower under salinity stress, supporting again the key role of roots in tolerating salinity. Lakra et al. [8] described high proline contents in IR64 (a salt-sensitive cultivar) and Pokkali (a salt-tolerant cultivar) under salinity stress, suggesting that this mechanism is not specific to salt-tolerant cultivars but is widespread across rice cultivars.

5. Conclusions

In this study, as in others that have evaluated salinity tolerance in *Saltol* accessions, the OsHKT1;5 protein was not detected even by shotgun proteomics, and it thus remains in doubt. Salt and PDX proteins, encoded in the *Saltol* QTL region, were detected in roots but only PDX was detected in shoots. In roots, the two proteins showed similar abundances between treatments but in shoots, PDX was increased under salinity stress. The study has created a large database for future studies of salinity-stress response in rice accessions harboring the *Saltol* region, comprising more than 2000 proteins expressed during the early stages of salinity stress in the shoots and roots of rice line FL478. Our dataset for root proteomic analysis is remarkable, as information about this tissue in the literature is very scarce and should be addressed as is the first barrier to avoid salinity excesses. Protein–protein interaction networks developed in this study allow identification of novel candidates of unknown function that may play major roles in tolerance to salinity stress, and invite further study. Among higher-abundance proteins, UnkS-13 and UnkS-1, involved respectively in amino acid synthesis and antioxidant stress, are potential candidates. Proteins UnkS-13 and UnkS-14, also showing higher abundance under salinity, are also promising. In roots, ROS scavenging

was crucial for salinity response, as was the maintenance of mitochondrial activity and amino acid metabolism. In shoots, there was also an activation of antioxidant machinery and of transcription mechanisms, though disparate and contrasting responses were observed for amino acid metabolism and the Calvin cycle. Stress-responsive proteins such as dehydrin and PLAT may play key roles, in view of their high activation during salinity stress. This study highlights the importance of examining both shoots and roots, because their salinity tolerance traits are different and respond to different requirements of the rice plant. It sheds light on adaptive processes under high salinity in rice plants and, in particular, in roots. This knowledge could be further used to develop highly tolerant rice cultivars.

CRedit authorship contribution statement

Camilo López-Cristoffanini: Visualization, methodology, formal analysis, writing - original draft. **Mireia Bundó:** Methodology, investigation, writing - review & editing. **Xavier Serrat:** Methodology, resources, investigation. **Blanca San Segundo:** Supervision, funding acquisition, writing - review & editing. **Marta López-Carbonell:** Supervision, writing - review & editing. **Salvador Nogués:** Funding acquisition, supervision, writing - review & editing.

Declaration of competing interest

The authors declare that they have no known competing financial interests or personal relationships that could have appeared to influence the work reported in this paper.

Acknowledgments

This project has received funding from the European Union's Horizon 2020 Research and Innovation Program under grant agreement No[678168]-NEURICE. The authors would also like to acknowledge the PFCHA Program of CONICYT for granting C.L. a BecasChile scholarship [72140224]. The authors are grateful for all the help provided by Javier Moros and all the people at the Plataforma de Proteómica del Parc Científic de Barcelona, a member of ProteoRed-ISCI.

Appendix A. Supplementary data

Supplementary data for this article can be found online at <https://doi.org/10.1016/j.cj.2020.10.009>.

References

- [1] I.N.B.L. Reddy, B. Kim, I. Yoon, K. Kim, T. Kwon, Salt tolerance in rice: focus on mechanisms and approaches, *Rice Sci.* 24 (2017) 123–144.
- [2] D.P. Heenan, L.G. Lewin, D.W. McCaffery, Salinity tolerance in rice varieties at different growth stages, *Aust. J. Exp. Agric.* 28 (1988) 343–349.
- [3] S. Abdollah Hosseini, J. Gharechahi, M. Heidari, P. Koobaz, S. Abdollahi, M. Mirzaei, B. Nakhoda, G. Hosseini Salekdeh, Comparative proteomic and physiological characterisation of two closely related rice genotypes with contrasting responses to salt stress, *Funct. Plant Biol.* 42 (2015) 527–542.
- [4] S. Negrão, M. Cecília Almadanim, I.S. Pires, I.A. Abreu, J. Maroco, B. Courtois, G. B. Gregorio, K.L. McNally, M. Margarida Oliveira, New allelic variants found in key rice salt-tolerance genes: an association study, *Plant Biotechnol. J.* 11 (2013) 87–100.
- [5] B. Gupta, B. Huang, Mechanism of salinity tolerance in plants: physiological, biochemical, and molecular characterization, *Int. J. Genomics* 2014 (2014) 701596.
- [6] P. Das, K.K. Nutan, S.L. Singla-Pareek, A. Pareek, Understanding salinity responses and adopting 'omics-based' approaches to generate salinity tolerant cultivars of rice, *Front. Plant Sci.* 6 (2015) 712.
- [7] K. Kumar, M. Kumar, S. Kim, H. Ryu, Y. Cho, Insights into genomics of salt stress response in rice, *Rice* 6 (2013) 27.

- [8] N. Lakra, C. Kaur, K. Anwar, S.L. Singla-Pareek, A. Pareek, Proteomics of contrasting rice genotypes: identification of potential targets for raising crops for saline environment, *Plant Cell Environ.* 1 (2017) 947–969.
- [9] S.J. Roy, S. Negrão, M. Tester, S.J. Roy, Salt resistant crop plants, *Curr. Opin. Biotechnol.* 26 (2014) 115–124.
- [10] M. Djanaguiraman, R. Ramadass, D.D. Devi, Effect of salt stress on germination and seedling growth in rice genotypes, *Madras Agric. J.* 90 (2003) 50–53.
- [11] J.D. Platten, J.A. Egdane, A.M. Ismail, Salinity tolerance, Na⁺ exclusion and allele mining of *HKT1;5* in *Oryza sativa* and *O. glaberrima*: many sources, many genes, one mechanism?, *BMC Plant Biol.* 13 (2013) 32.
- [12] H.X. Lin, M.Z. Zhu, M. Yano, J.P. Gao, Z.W. Liang, W.A. Su, X.H. Hu, Z.H. Ren, D. Y. Chao, QTLs for Na⁺ and K⁺ uptake of the shoots and roots controlling rice salt tolerance, *Theor. Appl. Genet.* 108 (2004) 253–260.
- [13] V. Kumar, A. Singh, S.V.A. Mithra, S.L. Krishnamurthy, S.K. Parida, S. Jain, K.K. Tiwari, P. Kumar, A.R. Rao, S.K. Sharma, J.P. Khurana, N.K. Singh, T. Mohapatra, Genome-wide association mapping of salinity tolerance in rice (*Oryza sativa*), *DNA Res.* 22 (2015) 133–145.
- [14] R.K. Singh, G.B. Gregorio, R.K. Jain, QTL Mapping for salinity tolerance in rice, *Physiol. Mol. Biol. Plants* 13 (2007) 87–99.
- [15] N.A. Eckardt, Sequencing the Rice Genome, *Plant Cell* 12 (2000) 2011–2017.
- [16] G. Zhang, Y. Guo, S. Chen, S. Chen, RFLP tagging of a salt tolerance gene in rice, *Rice Sci.* 110 (1995) 227–234.
- [17] J. Gong, P. He, Q. Qian, L. Shen, L. Zhu, S. Chen, Identification of salt-tolerance QTL in rice (*Oryza sativa* L.), *Chin.Sci.Bull.* 44 (1999) 68–71.
- [18] S.R. Prasad, G.B. Prashanth, S. Hittalmani, H.E. Shashidhar, Molecular mapping of quantitative trait loci associated with seedling tolerance to salt stress in rice (*Oryza sativa* L.), *Curr. Sci.* 78 (2000) 162–164.
- [19] M.L. Koyama, A. Levesley, R.M.D. Koebner, T.J. Flowers, A.R. Yeo, Quantitative trait loci for component physiological traits determining salt tolerance in rice, *Plant Physiol.* 125 (2001) 406–422.
- [20] P. Bonilla, J. Dvorak, D. Mackill, K. Deal, G. Gregorio, RFLP and SSLP mapping of salinity tolerance genes in chromosome 1 of rice (*Oryza sativa* L.) using recombinant inbred lines, *Philipp. Agric. Sci.* 85 (2002) 68–76.
- [21] G.B. Gregorio, D. Senadhira, R.D. Mendoza, N.L. Manigbas, J.P. Roxas, C.Q. Guerta, Progress in breeding for salinity tolerance and associated abiotic stresses in rice, *Field Crops Res.* 76 (2002) 91–101.
- [22] O. Cotsaftis, D. Plett, A.A.T. Johnson, H. Walia, C. Wilson, A.M. Ismail, T.J. Close, M. Tester, U. Baumann, Root-specific transcript profiling of contrasting rice genotypes in response to salinity stress, *Mol. Plant* 4 (2011) 25–41.
- [23] C. Sahi, A. Singh, K. Kumar, E. Blumwald, A. Grover, Salt stress response in rice: genetics, molecular biology, and comparative genomics, *Funct. Integr. Genomics* 6 (2006) 263–284.
- [24] M.J. Thomson, M. de Ocampo, J. Egdane, M.A. Rahman, A.G. Sajise, D.L. Adorada, E. Tumimbang-Raiz, E. Blumwald, Z.I. Seraj, R.K. Singh, G.B. Gregorio, A.M. Ismail, Characterizing the *Saltol* quantitative trait locus for salinity tolerance in rice, *Rice* 3 (2010) 148–160.
- [25] K.K. Nutan, H.R. Kushwaha, S.L. Singla-Pareek, A. Pareek, Transcription dynamics of *Saltol* QTL localized genes encoding transcription factors, reveals their differential regulation in contrasting genotypes of rice, *Funct. Integr. Genomics* 17 (2017) 69–83.
- [26] A. Waziri, P. Kumar, R.S. Purty, *Saltol* QTL and their role in salinity tolerance in rice, *Austin J. Biotechnol. Bioeng.* 29 (2016) 1067–1071.
- [27] S.L. Krishnamurthy, S.K. Sharma, V. Kumar, S. Tiwari, N.K. Singh, Analysis of genomic region spanning *Saltol* using SSR markers in rice genotypes showing differential seedlings stage salt tolerance, *J. Plant Biochem. Biotechnol.* 25 (2016) 331–336.
- [28] R. Samal, P.S. Roy, A.K. Dash, G.J.N. Rao, S. Bharathkumar, H.N. Subudhi, J.N. Reddy, Genetic diversity in the rice landraces (*Oryza sativa* L.) of coastal Sundarbans (India) and their adaptation to the local saline condition investigated both at molecular and physiological level, *Acta Physiol. Plant.* 38 (2016) 56.
- [29] S.H. Kim, P.R. Bhat, X. Cui, H. Walia, J. Xu, S. Wanamaker, A.M. Ismail, C. Wilson, T.J. Close, Detection and validation of single feature polymorphisms using RNA expression data from a rice genome array, *BMC Plant Biol.* 9 (2009) 65.
- [30] J.D. Platten, O. Cotsaftis, P. Berthomieu, H. Bohnert, R.J. Davenport, D.J. Fairbairn, T. Horie, R.A. Leigh, H.X. Lin, S. Luan, P. Mäser, O. Pantoja, A. Rodríguez-Navarro, D.P. Schachtman, J.I. Schroeder, H. Sentenac, N. Uozumi, A.A. Véry, J.K. Zhu, E.S. Dennis, M. Tester, Nomenclature for HKT transporters, key determinants of plant salinity tolerance, *Trends Plant Sci.* 11 (2006) 372–374.
- [31] B. Garciadeblás, M.E. Senn, M.A. Bañuelos, A. Rodríguez-Navarro, A.E. Senn, A. A. Ban, A. Rodrö, Sodium transport and HKT transporters: the rice model, *Plant J.* 34 (2003) 788–801.
- [32] R. Singh, N.S. Jwa, Understanding the responses of rice to environmental stress using proteomics, *J. Proteome Res.* 12 (2013) 4652–4669.
- [33] Z. Ren, J. Gao, L. Li, X. Cai, W. Huang, D. Chao, M. Zhu, Z. Wang, S. Luan, H. Lin, A rice quantitative trait locus for salt tolerance encodes a sodium transporter, *Nat. Genet.* 37 (2005) 1141–1146.
- [34] E. Balderas, D. Gollidack, H. Su, F. Quigley, U.R. Kamasani, C. Mun, O.V. Popova, J. Bennett, H.J. Bohnert, O. Pantoja, C. Muñoz-Garay, E. Balderas, O.V. Popova, J. Bennett, H.J. Bohnert, O. Pantoja, Characterization of a HKT-type transporter in rice as a general alkali cation transporter, *Plant J.* 31 (2002) 529–542.
- [35] H. Walia, C. Wilson, P. Condamine, X. Liu, A.M. Ismail, L. Zeng, S.I. Wanamaker, J. Mandal, J. Xu, X. Cui, T.J. Close, Comparative transcriptional profiling of two contrasting rice genotypes under salinity stress during the vegetative growth stage, *Plant Physiol.* 139 (2005) 822–835.
- [36] R. Mirdar Mansuri, Z.S. Shobbar, N. Babaeian Jelodar, M.R. Ghaffari, G.A. Nematzadeh, S. Asari, Dissecting molecular mechanisms underlying salt tolerance in rice: a comparative transcriptional profiling of the contrasting genotypes, *Rice* 12 (2019) 13.
- [37] N.I. Kobayashi, N. Yamaji, H. Yamamoto, K. Okubo, H. Ueno, A. Costa, K. Tanoi, H. Matsumura, M. Fujii-Kashino, T. Horiuchi, M.A. Nayef, S. Shabala, G. An, J.F. Ma, T. Horie, *OsHKT1;5* mediates Na⁺ exclusion in the vasculature to protect leaf blades and reproductive tissues from salt toxicity in rice, *Plant J.* 91 (2017) 657–670.
- [38] N.N. Babu, S.G. Krishnan, K.K. Vinod, S.L. Krishnamurthy, V.K. Singh, M.P. Singh, R. Singh, R.K. Ellur, V. Rai, H. Bollinedi, P.K. Bhowmick, A.K. Yadav, M. Nagarajan, N.K. Singh, K.V. Prabhu, A.K. Singh, Marker aided incorporation of *Saltol*, a major QTL associated with seedling stage salt tolerance, into *Oryza sativa* 'Pusa Basmati 1121', *Front. Plant Sci.* 8 (2017) 41.
- [39] R. Gupta, Y. Wang, G.K. Agrawal, R. Rakwal, I.H. Jo, K.H. Bang, S.T. Kim, Time to dig deep into the plant proteome: a hunt for low-abundance proteins, *Front. Plant Sci.* 6 (2015) 22.
- [40] M. Mirzaei, N. Soltani, E. Sarhadi, D. Pascovici, T. Keighley, G.H. Salekdeh, P.A. Haynes, B.J. Atwell, Shotgun proteomic analysis of long-distance drought signaling in rice roots, *J. Proteome Res.* 11 (2012) 348–358.
- [41] J.H. Cock, K.A. Gomez, *Laboratory Manual for Physiological Studies of Rice*, third ed., IRRI, Los baños, Laguna, the Philippines, 1976.
- [42] Y.J. Kim, H.M. Lee, Y. Wang, J. Wu, S.G. Kim, K.Y. Kang, K.H. Park, Y.C. Kim, I.S. Choi, G.K. Agrawal, R. Rakwal, S.T. Kim, Depletion of abundant plant RuBisCO protein using the protamine sulfate precipitation method, *Proteomics* 13 (2013) 2176–2179.
- [43] R. Gupta, S.T. Kim, Depletion of RuBisCO protein using the protamine sulfate precipitation method, in: A. Posch (Ed.), *Proteomic Profiling*, Humana Press, New York, USA, 2015, pp. 225–233.
- [44] Y. Suzuki, K. Nakabayashi, R. Yoshizawa, T. Mae, A. Makino, Differences in expression of the *RBCS* multigene family and rubisco protein content in various rice plant tissues at different growth stages, *Plant Cell Physiol.* 50 (2009) 1851–1855.
- [45] L. Käll, J.D. Storey, M.J. MacCoss, W.S. Noble, Assigning significance to peptides identified by tandem mass spectrometry using decoy databases, *J. Proteome Res.* 7 (2008) 29–34.
- [46] L. Käll, J.D. Canterbury, J. Weston, W.S. Noble, M.J. MacCoss, Semi-supervised learning for peptide identification from shotgun proteomics datasets, *Nat. Methods* 4 (2007) 923–925.
- [47] S.J. Callister, R.C. Barry, J.N. Adkins, E.T. Johnson, W. Qian, B.J.M. Webb-Robertson, R.D. Smith, M.S. Lipton, Normalization approaches for removing systematic biases associated with mass spectrometry and label-free proteomics, *J. Proteome Res.* 5 (2006) 277–286.
- [48] M. Kanehisa, S. Goto, KEGG: Kyoto Encyclopedia of Genes and Genomes, *Nucleic Acids Res.* 28 (2000) 27–30.
- [49] M. Kanehisa, Y. Sato, M. Kawashima, M. Furumichi, M. Tanabe, KEGG as a reference resource for gene and protein annotation, *Nucleic Acids Res.* 44 (2016) 457–462.
- [50] E. Oveland, T. Muth, E. Rapp, L. Martens, F.S. Berven, H. Barsnes, Viewing the proteome: How to visualize proteomics data?, *Proteomics* 15 (2015) 1341–1355.
- [51] P. Shannon, A. Markiel, O. Ozier, N.S. Baliga, J. Wang, D. Ramage, N. Amin, B. Schwikowski, T. Ideker, Cytoscape: a software environment for integrated models, *Genome Res.* 13 (2003) 2498–2504.
- [52] S.M. Cline, M. Smoot, E. Cerami, A. Kuchinsky, N. Landys, C. Workman, R. Christmas, I. Avila-campilo, M. Creech, B. Gross, K. Hanspers, R. Isserlin, R. Kelley, S. Killcoyne, S. Lotia, S. Maere, J. Morris, K. Ono, V. Pavlovic, A.R. Pico, A. Vailaya, P.-L. Wang, A. Adler, B.R. Conklin, L. Hood, M. Kuiper, C. Sander, I. Schumlevich, B. Schwikowski, G.J. Warner, T. Ideker, G.D. Bader, Integration of biological networks and gene expression data using Cytoscape, *Nat. Protoc.* 2 (2007) 2366–2382.
- [53] D. Szklarczyk, A.L. Gable, D. Lyon, A. Junge, S. Wyder, J. Huerta-Cepas, M. Simonovic, N.T. Doncheva, J.H. Morris, P. Bork, L.J. Jensen, C. Von Mering, STRING v11: protein-protein association networks with increased coverage, supporting functional discovery in genome-wide experimental datasets, *Nucleic Acids Res.* 47 (2019) D607–D613.
- [54] B.D. Halligan, S.P. Mirza, M.C. Pellitteri-hahn, M. Olivier, A.S. Greene, Visualizing quantitative proteomics datasets using treemaps, in: *Proceedings of the 11th International Conference Information Visualization, 2007*, pp. 637–648.
- [55] E.H. Baehrecke, N. Dang, K. Babaria, B. Shneiderman, Visualization and analysis of microarray and gene ontology data with treemaps, *BMC Bioinformatics* 5 (2004) 84.
- [56] A. Otto, J. Bernhardt, H. Meyer, M. Schaffer, F.A. Herbst, J. Siebourg, U. Mäder, M. Lalk, M. Hecker, D. Becher, Systems-wide temporal proteomic profiling in glucose-starved *Bacillus subtilis*, *Nat. Commun.* 1 (2010) 137.
- [57] M. Key, A tutorial in displaying mass spectrometry-based proteomic data using heat maps, *BMC Bioinf.* 13 (2012) S10.
- [58] Y. Benjamini, Y. Hochberg, Controlling the false discovery rate: a practical and powerful approach to multiple testing, *J. R. Stat. Soc. Ser. B* 57 (1995) 289–300.
- [59] R Core Team, R: A language and environment for statistical computing, R Foundation for Statistical Computing, Vienna, Austria, 2017. <https://www.r-project.org/>.

- [60] L.T.N. Huyen, L.M. Cuc, A.M. Ismail, L.H. Ham, Introgression the salinity tolerance QTLs *Saltol* into AS996, the elite rice variety of Vietnam, *Am. J. Plant Sci.* 3 (2012) 981–987.
- [61] A. Arzani, A.M. Rezai, R.K. Singh, G.B. Gregorio, Assessment of rice genotypes for salt tolerance using microsatellite markers associated with the *saltol*, *Afr. J. Biotechnol.* 7 (2008) 730–736.
- [62] M.H. Khan, S.K. Panda, Alterations in root lipid peroxidation and antioxidative responses in two rice cultivars under NaCl-salinity stress, *Acta Physiol. Plant.* 30 (2008) 81–89.
- [63] M. Kim, H. Kim, W. Lee, Y. Lee, S. Kwon, J. Lee, Quantitative shotgun proteomics analysis of rice anther proteins after exposure to high temperature, *Int. J. Genomics* 2015 (2015) 238704.
- [64] Y. Zhang, B.R. Fonslow, B. Shan, M.C. Baek, J.R. Yates III, Protein analysis by shotgun/bottom-up proteomics, *Chem. Rev.* 113 (2015) 213–223.
- [65] X. Li, M. Yang, Y. Zhu, Y. Liang, Proteomic analysis of salt stress responses in rice shoot, *J. Plant Biol.* 54 (2011) 384–395.
- [66] Z.Q. Wang, X.Y. Xu, Q.Q. Gong, C. Xie, W. Fan, J.L. Yang, Q.S. Lin, S.J. Zheng, Root proteome of rice studied by iTRAQ provides integrated insight into aluminum stress tolerance mechanisms in plants, *J. Proteomics* 98 (2014) 189–205.
- [67] Q. Xiong, L. Zhong, T. Shen, C. Cao, H. He, X. Chen, iTRAQ-based quantitative proteomic and physiological analysis of the response to N deficiency and the compensation effect in rice, *BMC Genomics* 20 (2019) 4.
- [68] N. Lakra, C. Kaur, S.L. Singla-Pareek, A. Pareek, Mapping the 'early salinity response' triggered proteome adaptation in contrasting rice genotypes using iTRAQ approach, *Rice* 12 (2019) 5.
- [69] C. Chu, N. Yan, Y. Du, X. Liu, M. Chu, J. Shi, H. Zhang, Y. Liu, Z. Zhang, iTRAQ-based proteomic analysis reveals the accumulation of bioactive compounds in Chinese wild rice (*Zizania latifolia*) during germination, *Food Chem.* 289 (2019) 635–644.
- [70] Q. Mu, W. Zhang, Y. Zhang, H. Yan, K. Liu, T. Matsui, X. Tian, P. Yang, iTRAQ-based quantitative proteomics analysis on rice anther responding to high temperature, *Int. J. Mol. Sci.* 18 (2017) 1811.
- [71] J. Ma, H. Sheng, X. Li, L. Wang, iTRAQ-based proteomic analysis reveals the mechanisms of silicon-mediated cadmium tolerance in rice (*Oryza sativa*) cells, *Plant Physiol. Biochem.* 104 (2016) 71–80.
- [72] S. Yan, Z. Tang, W. Su, W. Sun, Proteomic analysis of salt stress-responsive proteins in rice root, *Proteomics* 5 (2005) 235–244.
- [73] U. Deinlein, A.B. Stephan, T. Horie, W. Luo, G. Xu, J.I. Schroeder, Plant salt-tolerance mechanisms, *Trends Plant Sci.* 19 (2014) 371–379.
- [74] F. Moradi, A.M. Ismail, M. Manila, Responses of photosynthesis, chlorophyll fluorescence and ROS-scavenging systems to salt stress during seedling and reproductive stages in rice, *Ann. Bot.* 99 (2007) 1161–1173.
- [75] M. Zhu, J. Lin, J. Ye, R. Wang, C. Yang, J. Gong, Y. Liu, C. Deng, P. Liu, C. Chen, Y. Cheng, X. Deng, Y. Zeng, A comprehensive proteomic analysis of elaioplasts from citrus fruits reveals insights into elaioplast biogenesis and function, *Hortic. Res.* 5 (2018) 6.
- [76] J. Wan, S.D. Blakeley, D.T. Dennis, K. Ko, Transit peptides play a major role in the preferential import of proteins into leucoplasts and chloroplasts, *J. Biol. Chem.* 271 (1996) 31227–31233.
- [77] F.J.M. Maathuis, Sodium in plants: perception, signalling, and regulation of sodium fluxes, *J. Exp. Bot.* 65 (2014) 849–858.
- [78] M.C. Kim, W.S. Chung, D.J. Yun, M.J. Cho, Calcium and calmodulin-mediated regulation of gene expression in plants, *Mol. Plant* 2 (2009) 13–21.
- [79] S. Mahajan, G.K. Pandey, N. Tuteja, Calcium- and salt-stress signaling in plants: shedding light on SOS pathway, *Arch. Biochem. Biophys.* 471 (2008) 146–158.
- [80] S.K. Jami, G.B. Clark, B.T. Ayele, S.J. Roux, P.B. Kirti, Identification and characterization of annexin gene family in rice, *Plant Cell Rep.* 31 (2012) 813–825.
- [81] B. Qiao, Q. Zhang, D. Liu, H. Wang, J. Yin, R. Wang, M. He, M. Cui, Z. Shang, D. Wang, Z. Zhu, A calcium-binding protein, rice annexin OsANN1, enhances heat stress tolerance by modulating the production of H₂O₂, *J. Exp. Bot.* 66 (2015) 5853–5866.
- [82] C. Domingo, E. Lalanne, M.M. Catalá, E. Pla, J.L. Reig-Valiente, M. Talón, Physiological basis and transcriptional profiling of three salt-tolerant mutant lines of rice, *Front. Plant Sci.* 7 (2016) 1462.
- [83] Y.C. Park, S. Chapagain, C.S. Jang, A negative regulator in response to salinity in rice: *Oryza sativa* salt-, ABA- and drought-induced RING finger protein 1 (OsSADR1), *Plant Cell Physiol.* 59 (2018) 575–589.
- [84] M. Okamoto, F.C. Peterson, A. Defries, S.Y. Park, A. Endo, E. Nambara, B.F. Volkman, S.R. Cutler, Activation of dimeric ABA receptors elicits guard cell closure, ABA-regulated gene expression, and drought tolerance, *Proc. Natl. Acad. Sci. U. S. A.* 110 (2013) 12132–12137.
- [85] S. Karim, H. Aronsson, The puzzle of chloroplast vesicle transport-involvement of GTPases, *Front. Plant Sci.* 5 (2014) 472.
- [86] M. Alezzawi, Vesicle Transport in Chloroplasts with Emphasis on Rab Proteins, University of Gothenburg, Gothenburg, Sweden, 2004.
- [87] C. Lee, J. Goldberg, Structure of coatomer cage proteins and the relationship among COPI, COPII, and clathrin vesicle coats, *Cell* 142 (2010) 123–132.
- [88] A.R. Memon, The role of ADP-ribosylation factor and SAR1 in vesicular trafficking in plants, *Biochim. Biophys. Acta-Biomembr.* 1664 (2004) 9–30.
- [89] A. Baral, K.S. Shruithi, M.K. Mathew, Vesicular trafficking and salinity responses in plants, *IUBMB Life* 67 (2015) 677–686.
- [90] Y. Yang, W. Wang, Z. Chu, J. Zhu, H. Zhang, Roles of nuclear pores and nucleocytoplasmic trafficking in plant stress responses, *Front. Plant Sci.* 8 (2017) 574.
- [91] H. Feng, Q. Tang, J. Cai, B. Xu, G. Xu, L. Yu, Rice OsHAK16 functions in potassium uptake and translocation in shoot, maintaining potassium homeostasis and salt tolerance, *Planta* 250 (2019) 549–561.
- [92] Y. Leshem, L. Seri, A. Levine, Induction of phosphatidylinositol 3-kinase-mediated endocytosis by salt stress leads to intracellular production of reactive oxygen species and salt tolerance, *Plant J.* 51 (2007) 185–197.
- [93] M. Zwiewka, T. Nodzyński, S. Robert, S. Vanneste, J. Friml, Osmotic stress modulates the balance between exocytosis and clathrin-mediated endocytosis in *Arabidopsis thaliana*, *Mol. Plant* 8 (2015) 1175–1187.
- [94] A. Baral, N.G. Irani, M. Fujimoto, A. Nakano, S. Mayor, M.K. Mathew, Salt-induced remodeling of spatially restricted clathrin-independent endocytic pathways in *Arabidopsis* root, *Plant Cell* 27 (2015) 1297–1315.
- [95] Y. Luo, Z. Wang, H. Ji, H. Fang, S. Wang, L. Tian, X. Li, An *Arabidopsis* homolog of importin β 1 is required for ABA response and drought tolerance, *Plant J.* 75 (2013) 377–389.
- [96] A.D. Dooki, F.J. Mayer-Posner, H. Askari, Proteomic responses of rice young panicles to salinity, *Proteomics* 6 (2006) 6498–6507.
- [97] M. Hazman, B. Hause, E. Eiche, P. Nick, M. Riemann, Increased tolerance to salt stress in OPDA-deficient rice *ALLENE OXIDE CYCLASE* mutants is linked to an increased ROS-scavenging activity, *J. Exp. Bot.* 66 (2015) 3339–3352.
- [98] S. Wang, M. Cao, X. Ma, W. Chen, J. Zhao, C. Sun, L. Tan, F. Liu, Integrated RNA sequencing and QTL mapping to identify candidate genes from *Oryza rufipogon* associated with salt tolerance at the seedling stage, *Front. Plant Sci.* 8 (2017) 1427.
- [99] G. Verma, Y.V. Dhar, D. Srivastava, M. Kidwai, S. Chauhan, S.K. Bag, M.H. Asif, D. Chakrabarty, P.S. Chauhan, S.K. Bag, M.H. Asif, D. Chakrabarty, Genome-wide analysis of rice dehydrin gene family: its evolutionary conservedness and expression pattern in response to PEG induced dehydration stress, *PLoS ONE* 12 (2017) 1–22.
- [100] C. Wang, L.J. Zhang, R.D. Huang, Cytoskeleton and plant salt stress tolerance, *Plant Signal. Behav.* 6 (2011) 29–31.